Dual Degree Project

Stage III

Novel FVM - LBM method for compressible flows

Under the guidance of

Prof. Amit Agrawal

and

Prof. Bhalchandra Puranik

Submitted By:

Arpit Agarwal (02D10036)

5th Year Dual Degree Student

Mechanical Engineering Department

Indian Institute of Technology, Bombay

Powai, Mumbai-76

June. 2007.

Department of Mechanical Engineering

Indian Institute of Technology, Bombay

Acceptance Certificate

The Dual Degree Stage III report titled "**Novel FVM – LBM method for compressible flows"** submitted by **ARPIT AGARWAL** (Roll No. 02D10036) can be accepted for being evaluated.

Date: June 06, 2007

Prof. Amit Agrawal **Prof. B. Puranik**

Acknowledgement

I would like to express my eternal sincere thankfulness to Prof. Amit Agrawal, Prof. Bhalchandra Puranik and Prof. Chang Shu (NUS) for their guidance and valuable suggestions throughout the course of the project.

Date: June 06, 2007 **Arpit Agarwal**

Table of Contents

List of figures

List of Tables

Nomenclature

a	Sound speed
c	Particle velocity
e	Specific internal energy
E	Total internal energy
F	Flux vector
L	Reference Length
M	Molecular mass
P	Pressure
R	Gas constant
S	Wave speed
u_x	Velocity in x-direction
u_y	Velocity in y-direction
U	Vector of conserved variables
W	Vector of primitive variable
x	Distance in x-direction
y	Distance in y-direction
t	time
T	Temperature
ΔS	Surface area of the cell
ΔV	Volume of the cell
Δt	Time step
Δx	Distance between consecutive cells
ε	Knudsen number
γ	Specific heat ratio
η	Controlling parameter
ρ	Density

Subscripts

H	Head of the rarefaction wave
i	i^{th} cell
$i-\frac{1}{2}$	Cell face between i - 1 and i^{th} cell
ic	inter-cell
L	Left state
node	Node
R	Right state
t	Derivative with respect to time
T	Tail of the rarefaction wave
x	Derivative with respect to x
*	Property inside star region

Superscript

R	Reference state
^	Parameter in its dimensional form
0	Initial state
eq	Equilibrium
T	Transpose

Abbreviations

CFD	Computational Fluid Dynamics
FDM	Finite Difference Method
FEM	Finite Element Method
FVM	Finite Volume Method
LBM	Lattice Boltzmann Method

Abstract

Lattice Boltzmann Method (LBM) has developed as a new method in the field of Computational Fluid Dynamics and is a good alternative to the conventional numerical techniques like Finite Difference (FDM) and Finite Volume Method (FVM). The aim of this research work is to develop a novel robust FVM-LBM computational solver for compressible flows. The LBM model proposed by Kataoka and Tsutahara has been implemented in the new hybrid method which has been benchmarked for the following standard problems: shock tube problem (1D), shock expansion problem (2D), Roe Test and Riemann problem. The hybrid method has a higher computational efficiency and the results obtained with this method gives a steeper and more accurate shock profile as compared to the ones obtained by the FVM along with the widely used Godunov scheme. Finally, a thermodynamically consistent and fully conservative model for multi-component flows has been discussed and benchmarked for a few test cases. The new hybrid method has been used to simulate fluid flow having gases with different ratio of specific heat and molecular mass. It has been also observed that the hybrid method is more efficient than the pure FVM for multi-fluid flows.

Chapter 1

Introduction

Computational fluid dynamics (CFD) uses numerical methods and algorithms to solve and analyze problems that involve fluid flows. Computers can efficiently perform the calculations required to simulate engineering problems involving interaction of fluids and gases with the complex surfaces. So, computational simulations are often preferred over experimental methods to obtain higher accuracy and to minimize the time. Some of the commonly used numerical methods to solve differential equations are Finite Element Method (FEM), Finite Difference Method (FDM), Finite Volume Method (FVM) and Lattice Boltzmann Method (LBM). Each of these methods has its own relative advantages and disadvantages over others.

FEM is generally used for analysis in structural mechanics. CFD problems usually require discretization of the problem into a large number of cells, therefore computational cost favours simpler, lower order approximation within each cell. FEM may provide better accuracy but it proves to be too expensive for CFD problems. FDM is another numerical technique which approximates the partial differential equations to solve Navier-Stokes or Euler equations. This method is easy to implement but it is difficult to use FDM for unstructured meshes or complicated geometry.

In the finite volume method [1],[2], volume integrals in a partial differential equation that contain a divergence term are converted to surface integrals, using the divergence theorem. These terms are then evaluated as fluxes at the surfaces of each finite volume. "Finite volume" refers to the small volume surrounding each node point on a mesh. This method is conservative because the flux entering a given volume is identical to that leaving the adjacent volume. This method is commonly used in many CFD packages due to its several advantages.

FVM can also simulate shock waves and contact discontinuity waves due to its conservative nature. Another advantage of FVM is that this method can be easily formulated to allow for unstructured meshes. Numerical schemes have been proposed to compute the surface fluxes but the disadvantage of using FVM is that these schemes may be numerically expensive. Some of the approximate solvers for computing surface fluxes may be more efficient than the exact solver [2].

Lattice Boltzmann Method [3] has developed as an alternative and promising numerical technique for simulating fluid flows. Unlike the traditional methods which solve the Navier-Stokes and Euler Equations directly, this method is based upon solving mesoscopic kinetic equation (Boltzmann Equation) for the particle distribution function [3]. The fundamental idea in LBM is to construct a simplified kinetic model which obeys the Navier-Stokes or Euler equations. LBM has several advantages over other conventional CFD methods, especially in dealing with complex boundaries and algorithm parallelization. LBM has been also able to successfully simulate multi-fluid problems. Multi-fluid LBM models have been developed and these account for the increasing popularity of LBM in simulating complex fluid systems. LBM can also deal with complex boundary problems and can accurately simulate discontinuity waves like shock waves and contact discontinuity waves in compressible flow problems. But the biggest disadvantage of LBM is that it can not be used with non-uniform or unstructured meshes. Use of unstructured or non-uniform meshes is often desired to reduce computational time while simulating complex three-dimensional problem having a large domain of interest.

It has therefore been observed that Finite Volume Method and Lattice Boltzmann Method are the two numerical techniques which have been widely used in computational fluid dynamics due to their relative advantages over FEM and FDM. Both these methods also have some relative advantages and disadvantages over each other. LBM incorporates particle kinematics to accurately solve multi-fluid problems, but this method fails over non-uniform and unstructured meshes. Significant numerical diffusion has also been observed in some of the compressible flow models for LBM for e.g. the compressible flow model proposed by Kataoka and Tsutahara [4] with lower order discretization in space. On the other hand, FVM can be used with unstructured meshes, but it may be computationally expensive depending upon the numerical scheme used to compute the inter-cell fluxes. The relative advantages of these methods over each other provide a motivation to develop a novel hybrid FVM – LBM method which can incorporate the advantages of both FVM and LBM. A novel hybrid FVM – LBM method has been developed for compressible Euler equations in this work which is computationally efficient besides being more accurate than either of the two pure Finite volume and Lattice Boltzmann methods. This method can solve the multi-fluid flows which are relevant in nuclear power reactor safety analysis and also find applications in chemical engineering.

The plan of the thesis is as follows. Literature survey, which discusses the different numerical methods for compressible Euler equations along with their relative advantages and limitations over each other, has been presented in the chapter 2. Chapter 3 develops a theoretical background to analytically solve the Riemann problem. Solution of the local Riemann problem to obtain inter-cell parameters is a fundamental step in FVM. The widely used conventional numerical methods for solving compressible Euler equations have been discussed in the chapter 4. The novel FVM-LBM method for compressible flows has been introduced in the chapter 5. A numerical model for compressible multi-fluid flows has been discussed and the proposed hybrid FVM–LBM method has been extended to solve multi-fluid flows. The numerical model for the multi-fluid flows has been presented in the chapter 6. The results of the benchmarking tests have been presented and discussed in the chapter 7 and chapter 8.

Chapter 2

Literature Survey

Several models have been suggested in the literature to solve compressible Euler equations. The solution to the Euler equations may contain discontinuity waves such as shock waves and contact discontinuity waves. Such discontinuities pose some stringent requirements on the mathematical formulation of governing equations and the numerical schemes to solve the equations. Non-conservative formulations may fail at discontinuities and give wrong shock strength or shock speeds e.g. the one-dimensional shallow water equations [2]. It has been established that conservative numerical methods do converge to the weak solution of the conservation law [5].

Finite Volume Method is widely used to solve compressible Euler equations as this method is conservative and can simulate discontinuity waves. In FVM, volume integrals of the divergence terms in the partial differential equations are converted into surface integrals by Gauss-Divergence theorem and these terms are then evaluated as surface fluxes. Several schemes have been proposed in literature to obtain the surface parameters (or inter-cell parameters) from the given node parameters. Godunov scheme [2],[6] has been widely used to calculate the inter-cell parameters which are computed using analytical solution of local Riemann problems. Godunov scheme can accurately simulate discontinuity waves but this method has a high computational cost. Analytical solution to the local Riemann problem is obtained using iterative methods like Newton-Raphson method and this leads to an increased computational time. In a practical computation it may be required to solve the local Riemann problem billions of times, which makes the solution process a very demanding task in FVM.

Associated computational efforts with an iterative method may not always be justified. Approximate non-iterative solutions may have the potential to calculate the inter-cell parameters for the numerical purposes. Several approximate Riemann solvers have been proposed to find an approximation to a state and then evaluate the physical flux at this state. Some of these approximate solvers are exceedingly simple but they may not be accurate enough to produce robust numerical methods. The solver proposed by Roe [7] is one of the most well-known approximate Riemann solvers and has been applied to a very large variety of problems. Refinements to this approach were introduced by Roe and Pike [8] and the new methodology was simpler and more useful in solving Riemann problems. Corrections to the basic Roe scheme have been consistently made by experienced researchers but the solver may still fail to give desired accuracy in complicated cases. Harten, Lax and van Leer [9] proposed HLL Riemann solver which can directly approximate the inter-cell numerical fluxes without calculating the inter-cell parameters. The central idea of this method is two assume a two wave configuration which separates three constant states. This method is one of the very efficient and robust Riemann solvers but the limitation of this method is the assumption of two-wave configuration. As a consequence of this assumption, the resolution of physical features like contact discontinuity may be inaccurate. Modifications have been proposed to this solver [10], but the limitations of this method still remain.

Lattice Boltzmann Method [3] is another numerical method which is often used to simulate compressible flow problems with shock wave and discontinuity because of the advantage of high resolution for shock-wave computations. This method models fluid as consisting of particles which perform the consecutive processes of collision and propagation over a discrete lattice mesh. The numerical method has to confirm that macroscopic parameters (velocity, pressure, temperature and density) obtained by solving LBM satisfy the fluid dynamics equation (Euler Equation). Chapman-Enskog expansion [11] is the mathematical procedure which is used to confirm that LBM satisfies Euler equations. Several Lattice Boltzmann models have been proposed for incompressible Navier-Stokes equation. However the usual collision-propagation method employed in the incompressible model can not be used to solve the Euler equations as this method is limited to flows with small Mach number only. Earlier, the LBM was limited to low Mach number but in the recent years many compressible Lattice Boltzmann models have been proposed in the literature.

Alexander et al. [12] proposed a Lattice Boltzmann model with selectable sound speed to simulate compressible flow. In this model sound speed was set as low as possible by selecting the parameters of equilibrium distribution function properly. But this model failed to simulate compressible flows beyond a certain Mach number. Yu and Zhao [13] suggested another model in which sound speed is lowered by the introduction of an attractive force. Both of these models are isothermal models and cannot simulate temperature profiles and thus can not be used to develop robust compressible flow solvers. Guangwu, Yaosong and Shouxin [14] proposed a three-speed-three-energy-level Lattice Boltzmann model for compressible Euler equations. Specific heat ratio can be freely chosen in this 17-bit (a bit is the number of particle velocities or energy levels in a LBM model) thermal model, but this method is computationally expensive as it assumes three different levels of velocity and temperature. The results obtained from this model have been shown in figure 1. LBM for the compressible Euler Equation (2-dimensional) proposed by Kataoka and Tsutahara [4] is a 9-bit thermal model and is computationally less expensive than the three-speed-three-energy level model. This model has been discussed in detail in the following chapters.

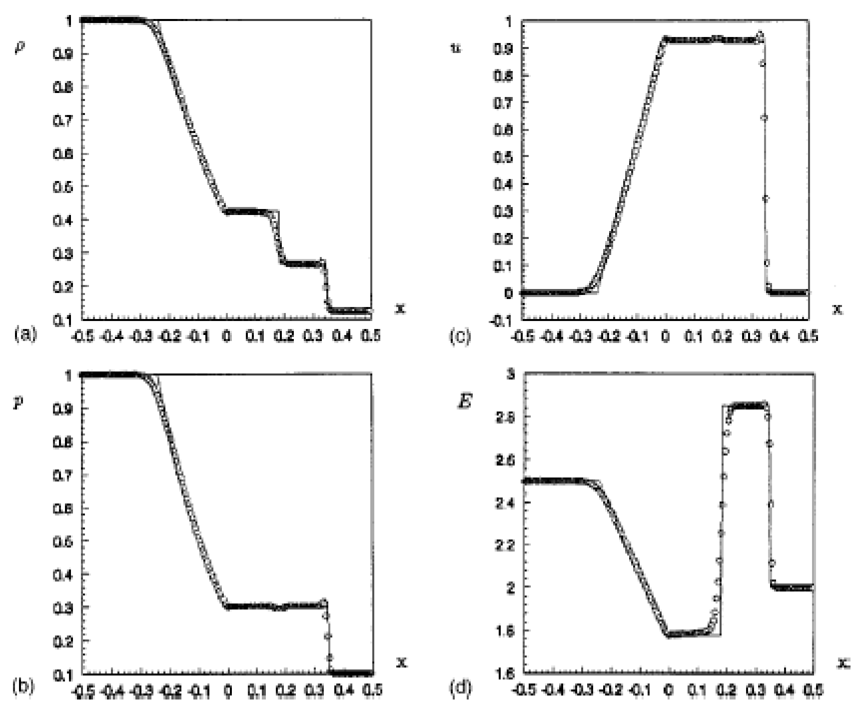

Fig 1: Results for a shock tube problem with a compressible flow LBM model [14]
(a). Density (b). Velocity (c). Pressure and (d). Internal energy

The two numerical techniques FVM and LBM have some relative advantages over each other and this provides a motivation to develop a novel hybrid FVM-LBM method for compressible flows. It has been observed that the new method is computationally efficient and simulates a steep and accurate shock profile as compared to the ones obtained by FVM along with the Godunov scheme. The new method will be discussed in detail in this thesis. The multi-fluid flows can also be successfully solved with this new numerical method. A comparison between the results obtained from the new numerical method and the multi-fluid FVM model proposed by Wang et al. will be made in the chapter 7.

Chapter 3

Exact solver to Riemann Problem

The one-dimensional time-dependent Euler equations with an ideal equation of state are studied in this chapter. The basic structure of the solution of the Riemann problem is also outlined along with a study of elementary waves present in the solution. Finally, exact solution to the Riemann problem is presented.

The conservative form of one-dimensional Euler equations in differential form is

$$U_t + F(U)_x = 0 \,. \tag{3.1}$$

Where U and F(U) are the vectors of conserved variables and fluxes given by

$$U = \begin{bmatrix} \rho \\ \rho u \\ E \end{bmatrix}, \; F(U) = \begin{bmatrix} \rho u \\ \rho u^2 + p \\ u(E+p) \end{bmatrix}. \tag{3.2}$$

Here ρ is density, p is pressure, u is velocity and E is total internal energy per unit volume given by

$$E = \rho(\frac{1}{2}u^2 + e) \tag{3.3}$$

where, e is the specific internal energy and it can be obtained by the equation of state for ideal gases.

$$e = e(p,\rho) = \frac{p}{(\gamma - 1)\rho}. \tag{3.4}$$

$\gamma = c_p / c_v$ denotes the ratio of specific heat.

The sound speed (a) is given by

$$a = \sqrt{\frac{\gamma p}{\rho}}\,. \tag{3.5}$$

Solution of the Riemann problem

Solution of the Riemann problem [2], [16] is a key ingredient of the conservative schemes to solve the Euler equations. The exact solution of Riemann problem is useful in a number of ways. The solution contains the fundamental physical and mathematical character of relevant set of conservation laws subject to the initial conditions. The exact Riemann problem solution is often used as a benchmarking case in assessing the performance of numerical methods. The solution of Riemann problem is used to simulate compressible Euler equations with Godunov scheme, which will be discussed in the next chapter. There is no closed-form solution to the Riemann problem and iterative schemes are used to arrive at the solution with a desired accuracy.

The Riemann problem for the one-dimensional time dependent Euler equations with data (U_L,U_R) is the initial value problem

$U_t + F(U)_x = 0$

$$U(x,0) = \begin{cases} U_L & \ldots\ldots\ldots \quad \text{if } x < 0 \\ U_R & \ldots\ldots\ldots \quad \text{if } x > 0 \,. \end{cases} \tag{3.6}$$

In the context of Euler equations, Riemann problem is a slight generalisation of the so called shock tube problem in which two stationary gases are separated by a diaphragm and the rupture of diaphragm generates a wave system. Elementary waves such as rarefaction waves, contact discontinuity waves and shock waves will be described and basic relations across these waves will be established. These relations are used to determine the complete solution of the Riemann problem. In Riemann problem, the initial state of gases need not be stationary.

1. Rarefaction wave: Rarefaction wave is a smooth wave across which all the parameters (density, velocity, pressure and internal energy) change. The wave has a fan-type shape and is enclosed by two bounding characteristics corresponding to the *Head* and *Tail* of the wave.
2. Contact discontinuity wave: This is a discontinuous wave across which pressure and velocity remains constant but density jumps discontinuously as do other density dependent variables like internal energy, temperature, sound speed, entropy, etc.
3. Shock wave: Shock waves are discontinuous waves across which all the parameters (density, velocity, pressure and internal energy) change.

Vector $W = (\rho,u,p)^T$ is more frequently used rather than the vector U in the solution of Riemann problem. Data consists of two constant states, which in terms of initial variables are $W_L = (\rho_L,u_L,p_L)^T$ to the left of x = 0 and $W_R = (\rho_R,u_R,p_R)^T$ to the right of x = 0, separated by a discontinuity at x = 0. For the case in which no vacuum is present (presence of vacuum is characterized by the condition $\rho = 0$), the exact solution of Riemann problem has three waves. These three waves separate our constant states which from the left to right are W_L (data on left hand side), W_{*L}, W_{*R}, and W_R (data on the right hand side). The unknown region between left and right waves is the '*Star Region*' which is separated into two sub-regions i.e. *Star left* (W_{*L}) and *Star right* (W_{*R}). The middle wave is always the contact discontinuity wave while the left and right waves may be shock or rarefaction waves. Therefore, there are four possible wave patterns which are mentioned in the table 1.

Table 1: Possible wave patterns in the solution of Riemann problem

Cases	Left wave	Right wave
Case 1	Rarefaction wave	Shock wave
Case 2	Shock wave	Rarefaction wave
Case 3	Rarefaction wave	Rarefaction wave
Case 4	Shock wave	Shock wave

Pressure (p_*) and velocity (u_*) do not vary across the contact discontinuity wave while the density takes two different values ρ_{*L} and ρ_{*R}. A solution procedure is now explained to compute the parameters in the *Star region*.

The solution for pressure (p_*) of the Riemann problem is given by the root of algebraic equation

$$f(p,W_L,W_R) \equiv f_L(p,W_L) + f_R(p,W_R) + u_R - u_L = 0 \tag{3.7}$$

where, the function f_L is given by

$$f_L(p,W_L) = \begin{cases} (p - p_L)\left[\dfrac{A_L}{p + B_L}\right]^{1/2} & \text{if } p > p_L \text{ (shock)} \\ \dfrac{2a_L}{\gamma - 1}\left[\left(\dfrac{p}{p_L}\right)^{\frac{\gamma-1}{2\gamma}} - 1\right] & \text{if } p \leq p_L \text{ (rarefaction)} \end{cases} \tag{3.8}$$

and the function f_R is given by

$$f_R(p,W_R)=\begin{cases}(p-p_R)\left[\dfrac{A_R}{p+B_R}\right]^{1/2} & \text{if } p > p_R \text{ (shock)}\\ \dfrac{2a_R}{\gamma-1}\left[\left(\dfrac{p}{p_R}\right)^{\frac{\gamma-1}{2\gamma}}-1\right] & \text{if } p \le p_R \text{ (rarefaction)}\end{cases} \tag{3.9}$$

and the data-dependent constants A_L, B_L, A_R, B_R are given by

$$A_L=\frac{2}{(\gamma+1)\rho_L},\quad B_L=\frac{(\gamma-1)}{(\gamma+1)}p_L,$$
$$A_R=\frac{2}{(\gamma+1)\rho_R},\quad B_R=\frac{(\gamma-1)}{(\gamma+1)}p_R. \tag{3.10}$$

The solution for velocity u_* is given by

$$u_*=\frac{1}{2}(u_L+u_R)+\frac{1}{2}[f_R(p_*)-f_L(p_*)]. \tag{3.11}$$

The unknown pressure p_* is obtained by solving the algebraic equation f(p) = 0. The behaviour of the function f(p), which is monotone and concave down plays a fundamental role in finding the equation roots numerically. The behaviour of the pressure function f(p) is particularly simple and analytical expression for the derivative of f(p) is also available. So Newton-Raphson iterative procedure is employed to find the root of f(p) = 0. A guess value p_0 is assumed for the true pressure p_*

$$p_0=\frac{1}{2}(p_L+p_R)-\frac{1}{8}(u_R-u_L)(a_L+a_R)(\rho_L+\rho_R) \tag{3.12}$$

and the corrected value obtained after the first iteration is given by

$$p_1=p_0-\frac{f(p_0)}{f'(p_0)}. \tag{3.13}$$

The above procedure generalized at the k-th iterate gives

$$p_k=p_{(k-1)}-\frac{f(p_{(k-1)})}{f'(p_{(k-1)})}. \tag{3.14}$$

Iterative procedure is stopped once the solution is within the desired tolerance range.

The above algorithm can compute p_* and u_*. The values of ρ_{*L} and ρ_{*R} are computed by identifying the types of non linear waves which is done by comparing the pressure p_* to the pressures p_L and p_R. The appropriate conditions are then applied across the left and right waves. Solution procedure to completely determine the left and right waves is also presented. The different possible cases are now considered to obtain the exact solution to the Riemann problem. These cases are taken from the references [2], [16].

Case 1: Left rarefaction wave and right shock wave ($p_* < p_L$ and $p_* > p_R$)

The three waves are: left rarefaction wave, contact discontinuity wave and right shock wave. The right shock wave is identified by the condition $p_* > p_R$. Density ρ_{*R} is obtained from the relation

$$\rho_{*R} = \rho_R \left[\frac{\frac{p_*}{p_R} + \frac{\gamma-1}{\gamma+1}}{\frac{\gamma-1}{\gamma+1}\frac{p_*}{p_R} + 1} \right] \tag{3.15}$$

and the shock wave speed S_R is computed using the relation

$$S_R = u_R + a_R \left[\frac{(\gamma+1)}{2\gamma}\frac{p_*}{p_R} + \frac{(\gamma-1)}{2\gamma} \right]^{1/2}. \tag{3.16}$$

The wave speed of contact discontinuity wave is $u*$.

The left rarefaction wave is identified by the condition $p_* < p_L$. The density ρ_{*L} is obtained from the relation

$$\rho_{*L} = \rho_L \left(\frac{p_*}{p_L}\right)^{1/\gamma}. \tag{3.17}$$

The rarefaction wave is enclosed by the *Head* and the *Tail*, and the speeds of these *Head* and *Tail* are given by

$$S_{HL} = u_L - a_L \quad \text{and} \quad S_{TL} = u_* - a_L \left(\frac{p_*}{p_L}\right)^{(\gamma-1)/2\gamma}. \tag{3.18}$$

The solution for $W_{Lfan} = (\rho,u,p)^T$ inside the rarefaction fan is given by

$$W_{Lfan} = \begin{cases} \rho = \rho_L \left[\dfrac{2}{(\gamma+1)} + \dfrac{(\gamma-1)}{(\gamma+1)a_L}(u_L - \dfrac{x}{t}) \right]^{2/(\gamma-1)}, \\ u = \dfrac{2}{(\gamma+1)} \left[a_L + \dfrac{(\gamma-1)}{2} u_L + \dfrac{x}{t} \right], \\ p = p_L \left[\dfrac{2}{(\gamma+1)} + \dfrac{(\gamma-1)}{(\gamma+1)a_L}(u_L - \dfrac{x}{t}) \right]^{2\gamma/(\gamma-1)}. \end{cases} \tag{3.19}$$

The complete solution set to this case is

$$W = \begin{cases} (\rho_L, u_L, p_L)^T & \text{if } x/t < S_{HL} \\ W_{Lfan} & \text{if } S_{HL} < x/t < S_{TL} \\ (\rho_{*L}, u_*, p_*)^T & \text{if } S_{TL} < x/t < u_* \\ (\rho_{*R}, u_*, p_*)^T & \text{if } u_* < x/t < S_R \\ (\rho_R, u_R, p_R)^T & \text{if } x/t > S_R \end{cases} \tag{3.20}$$

Case 2: Left shock wave and right rarefaction wave ($p_* > p_L$ and $p_* < p_R$)

The three waves are: left shock wave, contact discontinuity wave and right rarefaction wave. The right rarefaction wave is identified by the condition $p_* < p_R$. Density ρ_{*R} is obtained from the relation

$$\rho_{*R} = \rho_R \left(\frac{p_*}{p_R}\right)^{1/\gamma}. \tag{3.21}$$

The rarefaction wave is enclosed by the *Head* and the *Tail*, and the speeds of these *Head* and *Tail* are given by

$$S_{HR} = u_R + a_R \quad \text{and} \quad S_{TR} = u_* + a_R \left(\frac{p_*}{p_R}\right)^{(\gamma-1)/2\gamma}. \tag{3.22}$$

The solution for $W_{Rfan} = (\rho, u, p)^T$ inside the rarefaction fan is given by

$$W_{Rfan} = \begin{cases} \rho = \rho_R \left[\dfrac{2}{(\gamma+1)} - \dfrac{(\gamma-1)}{(\gamma+1)a_R}(u_R - \dfrac{x}{t}) \right]^{2/(\gamma-1)}, \\ u = \dfrac{2}{(\gamma+1)} \left[-a_R + \dfrac{(\gamma-1)}{2} u_R + \dfrac{x}{t} \right], \\ p = p_R \left[\dfrac{2}{(\gamma+1)} - \dfrac{(\gamma-1)}{(\gamma+1)a_R}(u_R - \dfrac{x}{t}) \right]^{2\gamma/(\gamma-1)}. \end{cases} \tag{3.23}$$

The wave speed of contact discontinuity wave is $u*$.

The left shock wave is identified by the condition $p_* > p_L$. The density ρ_{*L} is obtained from the relation

$$\rho_{*L} = \rho_L \left[\frac{\dfrac{p_*}{p_L} + \dfrac{\gamma-1}{\gamma+1}}{\dfrac{\gamma-1}{\gamma+1}\dfrac{p_*}{p_L} + 1} \right] \tag{3.24}$$

and the shock wave speed S_L is computed using the relation

$$S_L = u_L - a_L \left[\frac{(\gamma+1)}{2\gamma}\frac{p_*}{p_L} + \frac{(\gamma-1)}{2\gamma} \right]^{1/2}. \tag{3.25}$$

The complete solution set to this case is

$$W = \begin{cases} (\rho_L, u_L, p_L)^T & \text{if } x/t < S_L \\ (\rho_{*L}, u_*, p_*)^T & \text{if } S_L < x/t < u_* \\ (\rho_{*R}, u_*, p_*)^T & \text{if } u_* < x/t < S_{TR} \\ W_{Rfan} & \text{if } S_{TR} < x/t < S_{HR} \\ (\rho_R, u_R, p_R)^T & \text{if } x/t > S_{HR} \end{cases} \tag{3.26}$$

Case 3: Left rarefaction wave and right rarefaction wave ($p_* < p_L$ and $p_* < p_R$)

The three waves are: left rarefaction wave, contact discontinuity wave and right rarefaction wave. The right rarefaction wave is identified by the condition $p_* < p_R$. Density ρ_{*R} is obtained from the relation

$$\rho_{*R} = \rho_R \left(\frac{p_*}{p_R}\right)^{1/\gamma} . \tag{3.27}$$

The rarefaction wave is enclosed by the *Head* and the *Tail*, and the speeds of these *Head* and *Tail* are given by

$$S_{HR} = u_R + a_R \quad \text{and} \quad S_{TR} = u_* + a_R \left(\frac{p_*}{p_R}\right)^{(\gamma-1)/2\gamma} . \tag{3.28}$$

The solution for $W_{Rfan} = (\rho,u,p)^T$ inside the rarefaction fan is given by

$$W_{Rfan} = \begin{cases} \rho = \rho_R \left[\dfrac{2}{(\gamma+1)} - \dfrac{(\gamma-1)}{(\gamma+1)a_R}\left(u_R - \dfrac{x}{t}\right) \right]^{2/(\gamma-1)}, \\ u = \dfrac{2}{(\gamma+1)}\left[-a_R + \dfrac{(\gamma-1)}{2} u_R + \dfrac{x}{t} \right], \\ p = p_R \left[\dfrac{2}{(\gamma+1)} - \dfrac{(\gamma-1)}{(\gamma+1)a_R}\left(u_R - \dfrac{x}{t}\right) \right]^{2\gamma/(\gamma-1)}. \end{cases} \tag{3.29}$$

The wave speed of contact discontinuity wave is $u*$.

The left rarefaction wave is identified by the condition $p_* < p_L$. The density ρ_{*L} is obtained from the relation

$$\rho_{*L} = \rho_L \left(\frac{p_*}{p_L}\right)^{1/\gamma} . \tag{3.30}$$

The rarefaction wave is enclosed by the *Head* and the *Tail*, and the speeds of these *Head* and *Tail* are given by

$$S_{HL} = u_L - a_L \quad \text{and} \quad S_{TL} = u_* - a_L \left(\frac{p_*}{p_L}\right)^{(\gamma-1)/2\gamma} . \tag{3.31}$$

The solution for $W_{Lfan} = (\rho,u,p)^T$ inside the rarefaction fan is given by

$$W_{Lfan} = \begin{cases} \rho = \rho_L \left[\dfrac{2}{(\gamma+1)} + \dfrac{(\gamma-1)}{(\gamma+1)a_L}(u_L - \dfrac{x}{t}) \right]^{2/(\gamma-1)}, \\ u = \dfrac{2}{(\gamma+1)} \left[a_L + \dfrac{(\gamma-1)}{2} u_L + \dfrac{x}{t} \right], \\ p = p_L \left[\dfrac{2}{(\gamma+1)} + \dfrac{(\gamma-1)}{(\gamma+1)a_L}(u_L - \dfrac{x}{t}) \right]^{2\gamma/(\gamma-1)}. \end{cases} \tag{3.32}$$

The complete solution set to this case is

$$W = \begin{cases} (\rho_L, u_L, p_L)^T & \text{if } x/t < S_{HL} \\ W_{Lfan} & \text{if } S_{HL} < x/t < S_{TL} \\ (\rho_{*L}, u_*, p_*)^T & \text{if } S_{TL} < x/t < u_* \\ (\rho_{*R}, u_*, p_*)^T & \text{if } u_* < x/t < S_{TR} \\ W_{Rfan} & \text{if } S_{TR} < x/t < S_{HR} \\ (\rho_R, u_R, p_R)^T & \text{if } x/t > S_{HR} \end{cases} \tag{3.33}$$

Case 4: Left shock wave and right shock wave ($p_* > p_L$ and $p_* > p_R$)

The three waves are: left shock wave, contact discontinuity wave and right shock wave. The right shock wave is identified by the condition $p_* > p_R$. The density ρ_{*R} is obtained from the relation

$$\rho_{*R} = \rho_R \left[\frac{\dfrac{p_*}{p_R} + \dfrac{\gamma-1}{\gamma+1}}{\dfrac{\gamma-1}{\gamma+1}\dfrac{p_*}{p_R} + 1} \right] \tag{3.34}$$

and the shock wave speed S_R is computed using the relation

$$S_R = u_R + a_R \left[\frac{(\gamma+1)}{2\gamma}\frac{p_*}{p_R} + \frac{(\gamma-1)}{2\gamma} \right]^{1/2}. \tag{3.35}$$

The wave speed of contact discontinuity wave is $u*$.

The left shock wave is identified by the condition $p_* > p_L$. Density ρ_{*L} is obtained from the relation

$$\rho_{*L} = \rho_L \left[\frac{\frac{p_*}{p_L} + \frac{\gamma-1}{\gamma+1}}{\frac{\gamma-1}{\gamma+1}\frac{p_*}{p_L} + 1} \right] \tag{3.36}$$

and the shock wave speed S_L is computed using the relation

$$S_L = u_L - a_L \left[\frac{(\gamma+1)}{2\gamma}\frac{p_*}{p_L} + \frac{(\gamma-1)}{2\gamma} \right]^{1/2} . \tag{3.37}$$

The complete solution set to this case is

$$W = \begin{cases} (\rho_L, u_L, p_L)^T & \text{if } x/t < S_L \\ (\rho_{*L}, u_*, p_*)^T & \text{if } S_L < x/t < u_* \\ (\rho_{*R}, u_*, p_*)^T & \text{if } u_* < x/t < S_R \\ (\rho_R, u_R, p_R)^T & \text{if } x/t > S_R \end{cases} \tag{3.38}$$

The computational solver has been developed to find the exact solution of the complete wave structure of the Riemann problem at any point in the relevant domain of interest and at a time t > 0. This solver forms an important part of the Godunov scheme, which will be discussed in the following chapter.

Chapter 4

Numerical methods for compressible Euler equations

This chapter discusses the numerical methods which have been widely used to solve the compressible Euler equations. The methods are

a. Finite Volume Method (FVM) along with the use of Godunov scheme to obtain the inter-cell parameters.
b. Lattice Boltzmann Method (LBM)

4.1 FVM along with the Godunov scheme for compressible Euler equations

The finite volume method [1], [2] is a numerical method for solving partial differential equations that calculates the values of the conserved variables averaged across a volume. This fully conservative method overcomes some of the limitations of FDM. The use of integral form of the differential equations gives greater flexibility in solving complicated boundary problems, as the finite volumes need not be regular. The method also works with unstructured grids which is another limitation of FDM.

The three-dimensional Euler equations are of the form

$$U_t + \nabla.[F(U)] = 0 \tag{4.1}$$

where $F(U)$ is the flux vector.

These equations in an arbitrary domain of volume V and bounded by a closed surface S can be expressed in the following integral form as

$$\frac{\partial}{\partial t}\int_V U dV + \nabla.\int_V F dV = 0 . \tag{4.2}$$

The volume integral containing the divergence term is converted to the surface integral using the Gauss divergence theorem. Therefore, the modified integral form is

$$\frac{\partial}{\partial t}\int_V U dV + \int_S F dS = 0 . \tag{4.3}$$

The integral conservation equation is not only applicable to the entire problem domain, but it is also applicable to each control volume. Global conservation equations can be simply obtained by summing up the conservation equation of each control volume. Thus global conservation is built into the method and this is one of the advantages of the FVM.

The surface and volume integrals need to be approximated. To exactly compute the surface integral the flux value *F* everywhere on the surface S will be required, which is not known. The mean flux value over the surface is approximated as the inter-cell flux. Thus the surface integral is given as

$$\int_S F dS = F(U)_{ic}\Delta S \tag{4.4}$$

Subscript (*ic*) denotes inter-cell and ΔS is the surface area of the cell.

Similarly the volume integral is obtained by approximating the integrand U at the node. Thus the volume integral is given as

$$\int_V U dV = U_{node}\Delta V \tag{4.5}$$

Subscript (*node*) denotes node and ΔV is the volume of the cell.

The conservative discretized form of the equation (4.3) can therefore be used to solve compressible Euler equation by Finite Volume method.

The one-dimensional Euler equations, which have been studied in the previous chapter, is of the form $U_t + F(U)_x = 0$. (4.6)

A conservative FVM scheme for the one-dimensional Euler equations is of the form

$$U_i^{n+1} = U_i^n + \frac{\Delta t}{\Delta x}\left[F_{i-½} - F_{i+½}\right] \tag{4.7}$$

where, U_i^n denotes the parameters at the node i and at time interval n.

Godunov scheme [2],[6] is a widely used conservative numerical scheme for solving partial differential equations. This scheme computes the inter-cell parameters by using the solution of local Riemann problem. A basic assumption in Godunov scheme is that the data has a piece-wise linear distribution and parameter values in between the two inter-cells are assumed to be equal to the node parameter values. The data at time level n may be seen as pairs of constant states (U_i^n, U_{i+1}^n) separated by a discontinuity at the inter-cell boundary $x_{i+½}$. Thus the local Riemann problem is defined as

PDE: $U_t + F(U)_x = 0$

Initial Condition: $U(x,0) = U_i^n$ ……... if $x < 0$

U_{i+1}^n ……... if $x > 0$. (4.8)

This local Riemann problem is analytically solved using the exact solver for Riemann problem, which was discussed in the previous chapter. The analytical solution of this local Riemann problem at location x = 0 corresponds to the inter-cell parameters $U_{i+½}$. The inter-cell fluxes $F_{i-½}$ and $F_{i+½}$ are given by

$$F_{i-½} = F(U_{i-½}) \text{ and } F_{i+½} = F(U_{i+½}). \qquad (4.9)$$

The solution of the global problem at the next time step (n+1) is then obtained by substituting the fluxes in the conservative form of Euler equations. This is a widely used method for the simulating Euler equations. But, the analytical solution for local Riemann problem is obtained by iterative methods like Newton-Raphson method and this reduces the computational efficiency of the Godunov solver. The chapter 5 will introduce a new FVM - LBM method to overcome this drawback.

4.2 LBM for compressible Euler equations

The fundamental idea in Lattice Boltzmann Method is to construct a simplified kinetic model which obeys the Navier-Stokes or Euler equations. This method is based upon solving the Boltzmann Equation for the particle distribution function [3]. LBM has some important features which distinguishes it from other numerical method. Some of the features of conventional Lattice Boltzmann method are:

1. The Navier-Stokes or Euler equation can be obtained by Chapman-Enskog expansion [11],[17].

2. A minimum set of velocities are chosen and the fundamental particles are expected to move in those directions only [3].

3. The Bhatnagar-Gross-Krook collision model [18] is applied to the Boltzmann equation.

The conventional LBM model for can not simulate flow with high Mach numbers and also generates some severe oscillations near the discontinuities which can not be removed easily. These limitations of conventional LBM model, which normally solves the Navier-Stokes equation, provided a motivation to study alternate LBM models suitable for compressible Euler equations. The model proposed by Kataoka and Tsutahara [4] can solve the inviscid Euler equations. This model can simulate steep shock profiles and contact discontinuities encountered in the benchmarking problems. This model overcomes the defect in some of the previously used models [11],[17] that the specific heat ratio of the gas cannot be freely chosen.

Variables and equations are expressed in their non-dimensional form for the convenience of numerical calculations and analysis. The non dimensional variables and equations for the following analysis are first listed below. Let $L, \hat{\rho}^R$, $\hat{T}^R$ be the reference length, density and temperature, respectively. The corresponding non dimensional variables are defined as:

$$
\begin{aligned}
& t = \frac{\hat{t}}{L/\sqrt{R\hat{T}^R}}, x = \frac{\hat{x}}{L}, y = \frac{\hat{y}}{L}, c_{xi} = \frac{\hat{c}_{xi}}{\sqrt{R\hat{T}^R}}, c_{yi} = \frac{\hat{c}_{yi}}{\sqrt{R\hat{T}^R}}, \eta_i = \frac{\hat{\eta}_i}{\sqrt{R\hat{T}^R}}, \\
& f_i = \frac{\hat{f}_i}{\hat{\rho}^R}, f_i^{eq} = \frac{\hat{f}_i^{eq}}{\hat{\rho}^R}, \\
& \rho = \frac{\hat{\rho}}{\hat{\rho}^R}, u_x = \frac{\hat{u}_x}{\sqrt{R\hat{T}^R}}, u_y = \frac{\hat{u}_y}{\sqrt{R\hat{T}^R}}, T = \frac{\hat{T}}{\hat{T}^R}, p = \frac{\hat{p}}{\hat{\rho}^R R\hat{T}^R}, \\
& \rho^0 = \frac{\hat{\rho}^0}{\hat{\rho}^R}, u_x^0 = \frac{\hat{u}_x^0}{\sqrt{R\hat{T}^R}}, u_y^0 = \frac{\hat{u}_y^0}{\sqrt{R\hat{T}^R}}, T^0 = \frac{\hat{T}^0}{\hat{T}^R}, p^0 = \frac{\hat{p}^0}{\hat{\rho}^R R\hat{T}^R}.
\end{aligned}
\tag{4.10}
$$

The compressible Euler Equations and their initial conditions in terms of non dimensional variables are:

$$\frac{\partial \rho}{\partial t} + \frac{\partial \rho u_x}{\partial x} + \frac{\partial \rho u_y}{\partial y} = 0,$$

$$\frac{\partial \rho u_x}{\partial t} + \frac{\partial \rho u_x^2}{\partial x} + \frac{\partial \rho u_x u_y}{\partial y} + \frac{\partial p}{\partial x} = 0 ,$$

$$\frac{\partial \rho u_y}{\partial t} + \frac{\partial \rho u_x u_y}{\partial x} + \frac{\partial \rho u_y^2}{\partial y} + \frac{\partial p}{\partial y} = 0 ,$$

$$\frac{\partial \rho (bT + u_x^2 + u_y^2)}{\partial t} + \frac{\partial \rho u_x (bT + u_y^2) + 2pu_x}{\partial x} + \frac{\partial \rho u_y (bT + u_x^2) + 2pu_y}{\partial y} = 0 ,$$

$$p = \rho T . \tag{4.11}$$

where t is non-dimensional time, x and y are non-dimensional spatial coordinates, ρ, u_x, u_y, R, T and p are respectively non dimensional density, flow velocity in x-direction, flow velocity in y-direction, gas constant, temperature and pressure. f_i and f_{ieq} are the particle velocity distribution function and the equilibrium particle velocity distribution function respectively. The symbol with (^) indicates the same quantities in their dimensional forms. b is a constant which is expressed in terms of specific heat ratio (γ) as

$$b = 2/(\gamma - 1) \tag{4.12}$$

The initial condition is described as

$$\rho = \rho_0, u_x = u_x^0, u_y = u_y^0, T = T^0 \qquad \text{at } t = 0. \tag{4.13}$$

The macroscopic variables density, velocity and temperature are defined in terms of particle distribution function as:

$$\rho = \sum_{i=1}^{I} f_i,$$

$$\rho u_x = \sum_{i=1}^{I} f_i c_{xi},$$

$$\rho u_y = \sum_{i=1}^{I} f_i c_{yi},$$

$$\rho (bT + u_x^2 + u_y^2) = \sum_{i=1}^{I} f_i (c_{xi}^2 + c_{yi}^2 + \eta_i^2). \tag{4.14}$$

c_{xi} and c_{yi} are the molecular velocities of the particle moving in ith direction (i = 1,2…. I=9) and variable η_i has been introduced to control the specific heat ratio.

The kinetic equation and its initial condition of non dimensional form are

$$\frac{\partial f_i}{\partial t} + c_{xi}\frac{\partial f_i}{\partial x} + c_{yi}\frac{\partial f_i}{\partial y} = \frac{f_i^{eq}(\rho, u_x, u_y, T) - f_i}{\varepsilon} \tag{4.15}$$

and $$f_i = f_i^{eq}(\rho^0, u_x{}^0, u_y{}^0, T^0) \tag{4.16}$$

where, ε is the Knudsen Number.

The two dimensional Lattice Boltzmann Model proposed by Kataoka and Tsutahara has been presented below.

$$(c_{xi}, c_{yi}) = \begin{cases} (0,0) & \text{for i =1} \\ v_1(\cos\frac{\Pi i}{2}, \sin\frac{\Pi i}{2}) & \text{for i = 2,3,4,5} \\ v_2(\cos\frac{\Pi(i+.5)}{2}, \sin\frac{\Pi(i+.5)}{2}) & \text{for i = 6,7,8,9} \end{cases} \tag{4.17}$$

$$\text{and, } \eta_i = \begin{cases} \eta_0 & \text{for i = 1} \\ 0 & \text{for i = 2,3,...9} \end{cases} \tag{4.18}$$

where v_1, v_2 ($v_1 \neq v_2$) and η_0 are non-zero constants.

The local equilibrium velocity distribution function is defined as

$$f_i^{eq} = \rho(A_i + B_i(u_x c_{xi} + u_y c_{yi}) + D_i(u_x c_{xi} + u_y c_{yi})^2) \quad \text{for i = 1,2...9} \tag{4.19}$$

where,

$$A_i = \begin{cases} \frac{b-2}{\eta_0^2}T & \text{for i =1} \\ \frac{1}{4(v_1^2 - v_2^2)}\left[-v_2^2 + ((b-2)\frac{v_2^2}{\eta_0^2} + 2)T + \frac{v_2^2}{v_1^2}(u_x^2 + u_y^2)\right] & \text{for i =2,3,4,5} \\ \frac{1}{4(v_2^2 - v_1^2)}\left[-v_1^2 + ((b-2)\frac{v_1^2}{\eta_0^2} + 2)T + \frac{v_1^2}{v_2^2}(u_x^2 + u_y^2)\right] & \text{for i =6,7,8,9} \end{cases}, \tag{4.20}$$

$$B_i = \begin{cases} \frac{-v_2^2 + (b+2)T + u_x^2 + u_y^2}{2v_1^2(v_1^2 - v_2^2)} & \text{for i = 2,3,4,5} \\ \frac{-v_1^2 + (b+2)T + u_x^2 + u_y^2}{2v_2^2(v_2^2 - v_1^2)} & \text{for i = 6,7,8,9} \end{cases}, \tag{4.21}$$

$$D_i = \begin{cases} \dfrac{1}{2v_1^4} & \text{for } i = 2,3,4,5 \\ \dfrac{1}{2v_2^4} & \text{for } i = 6,7,8,9 \end{cases} . \tag{4.22}$$

The parameters in equations (4.17) and (4.18) are chosen to be $v_1 = 1$, $v_2 = 3$, $\eta_0 = 2$. The finite difference scheme with the usual first-order forward in time and second-order upwind in space is used for numerical computations of the Boltzmann equation. This model is simpler and numerically less expensive then some of the previously proposed models.

Chapter 5

New FVM - LBM method for Euler Equation

As discussed in the previous chapter, FVM along with the use of Godunov scheme, to calculate the inter-cell parameters, is a widely used numerical method to solve compressible Euler equations. This is a conservative numerical method and will converge to the weak form of solution to the Euler equations even at discontinuities. But the disadvantage of the method is that the inter-cell parameters are obtained form the node-parameters by analytically solving the Riemann problem. The analytical solution of local Riemann problem in-turn is obtained using iterative method which will make the computations expensive. Also, it is not always required to attain a very high accuracy in simulating the inter-cell parameters, therefore the use of Godunov scheme may not always be recommended. LBM is another numerical method which is widely used to solve compressible Euler equations. This method is computationally efficient and can be easily implemented to solve compressible fluid flows. LBM can also be very effective in simulating multi-fluid flows. But the biggest disadvantage of LBM is that LBM can not be used with unstructured and non-uniform meshes.

The limitations of FVM and LBM provide a motivation to generate a new hybrid FVM-LBM method for Euler equations which can incorporate the advantages of both FVM and LBM. This new method has been generated from the same fundamental idea as in Godunov scheme. Godunov scheme is a conventional and widely used scheme for compressible Euler equations to obtain the inter-cell macroscopic parameter values from the node parameters. These inter-cell parameters are required to calculate flux at the interface.

The new method uses LBM proposed by Kataoka and Tsutahara [4] to simulate the inter-cell parameters at the new time step from the known cell and inter-cell parameters at the earlier time step. The solution procedure in the new method is non-iterative and is more efficient than Godunov scheme where the solution procedure is iterative. The conservative FVM can then be used to calculate the node parameters. The grid for the new scheme is shown in the figure 2.

X		X		X	
.	o	.	o	.	o
X		X		X	
.	o	.	o	.	o
X		X		X	
.	o	.	o	.	o

Fig 2: Grid structure of a 2-dimensional problem indicating node and inter-cell points

Here (.) indicates node point and (o) and (X) are X and Y inter-cell points respectively. The steps implemented in the computational solver for the new numerical scheme are:

1. Parameter values at the old time step are assigned to each node and inter-cell.

2. The macroscopic parameter values are obtained for the X and Y inter-cell at the next time step by implementing the LBM model proposed by Kataoka and Tsutahara. The calculation of parameters at each of these points requires the solution of local Riemann problem by the LBM model. The corresponding grids on which LBM is applied for one time step are shown in figure 3.

(a).

.	o	.
.	o	.
.	o	.
LN	XI	RN

and

(b).

.	.	.	TN
X	X	X	YI
.	.	.	BN

Fig 3: (a). Grid structure for obtaining the x inter-cell parameter values by LBM.
(b). Grid structure for obtaining the y inter-cell parameter values by LBM.

where,

LN	Left Node		TN	Top Node
XI	X inter-cell	(inter-cell parameters have to be computed)	YI	Y inter-cell
RN	Right Node		BN	Bottom Node

3. The fluxes are calculated at each inter-cell from the inter-cell parameter values calculated using LBM.

4. The conservative FVM scheme which has been discussed in the chapter 4 is solved to obtain the node parameters at the new time step.

Benchmarking of this method has been done with several standard test cases as discussed in the chapter 7. A comparison of the results obtained and the computational time required with the new FVM – LBM method and FVM (along with the use of Godunov scheme) is also done in the chapter 7.

Chapter 6

Model for compressible multi-fluid flows

The numerical simulation of multi-component or multi-fluid flows has recently received a great deal of attention. Such flows are relevant in nuclear power reactor safety analysis and find applications in chemical engineering and petroleum industries. A thermodynamically consistent and fully conservative treatment of contact discontinuities has been proposed by Wang et al. [15] for the simulation of compressible multi-component flows. This treatment is able to accurately capture the contact discontinuities. FVM along with Godunov scheme has been widely used for the simulation of single-fluid flow Euler equations, but Euler equations alone can not be used to solve complicated multi-fluid flows. An extended conservation system with additional conservational equations beside the original Euler equations has been introduced in the new model. The additional equations describe the conservation of parameters like mass fraction of each component of the gas and the ratio of specific heats of the mixture (γ). The proposed model is simple, physically consistent, fully conservative and independent of the type of numerical schemes used to implement it.

Wang et al. [15] derived a new conservative model based upon the concept of total energy conservation of the mixture. This model involves two new formulations for the calculation of the ratio of specific heats of the mixture (γ) and the molecular weight of the mixture (M) in addition to the Euler equations. These new formulations are

$$\frac{\partial}{\partial t}(\frac{1}{M}\rho) + \nabla.(\frac{1}{M}\rho u) = 0 \tag{6.1}$$

and $$\frac{\partial}{\partial t}(\chi\rho) + \nabla.(\chi\rho u) = 0 \tag{6.2}$$

where, χ is the ratio of specific heat at constant pressure to the gas constant, i.e.

$$\chi = \frac{\gamma}{(\gamma - 1)} \ . \tag{6.3}$$

Therefore the complete model including the new equations is

$$U_t + F(U)_x = 0 \ . \tag{6.4}$$

where U and F(U) are the vectors of conserved variables and fluxes given by

$$U = \begin{bmatrix} \rho \\ \rho u \\ E \\ \rho / M \\ \chi\rho \end{bmatrix}, \quad F(U) = \begin{bmatrix} \rho u \\ \rho u^2 + p \\ u(E+p) \\ \rho u / M \\ \chi\rho u \end{bmatrix} \ . \tag{6.5}$$

A computational solver has been developed to simulate multi-fluid flow using the proposed model. Godunov scheme is employed to calculate the inter-cell parameters which are required to calculate the inter-cell flux. This model has also been benchmarked against a few test cases which have been discussed in the results chapter. Godunov scheme suffers from similar limitations which have been discussed earlier. Use of iterative methods to compute analytical solution increases computational time and makes the solver less efficient.

Finally, we propose to use the new hybrid FVM-LBM method which was introduced in the chapter 5 instead of the usual FVM (along with Godunov scheme) to reduce the computational time and to accurately simulate shock profile. LBM proposed by Kataoka and Tsutahara can be used for gases with variable specific heat ratio and molecular masses. Non-dimensional variables are defined in terms of the reference length (L), reference density ($\hat{\rho}^R$), reference gas constant ($\hat{R}^R$) and reference temperature ($\hat{T}^R$). The new set of non – dimensional variables for multi-fluid flows is

$$t = \frac{\hat{t}}{L / \sqrt{\hat{R}^R \hat{T}^R}}, x = \frac{\hat{x}}{L}, y = \frac{\hat{y}}{L}, c_{xi} = \frac{\hat{c}_{xi}}{\sqrt{\hat{R}^R \hat{T}^R}}, c_{yi} = \frac{\hat{c}_{yi}}{\sqrt{\hat{R}^R \hat{T}^R}}, \eta_i = \frac{\hat{\eta}_i}{\sqrt{\hat{R}^R \hat{T}^R}},$$

$$f_i = \frac{\hat{f}_i}{\hat{\rho}^R}, f_i^{eq} = \frac{\hat{f}_i^{eq}}{\hat{\rho}^R},$$

$$
\begin{aligned}
&\rho = \frac{\hat{\rho}}{\hat{\rho}^R}, u_x = \frac{\hat{u}_x}{\sqrt{\hat{R}^R \hat{T}^R}}, u_y = \frac{\hat{u}_y}{\sqrt{\hat{R}^R \hat{T}^R}}, RT = \frac{\hat{R}\hat{T}}{\hat{R}^R \hat{T}^R}, p = \frac{\hat{p}}{\hat{\rho}^R \hat{R}^R \hat{T}^R}, \\
&\rho^0 = \frac{\hat{\rho}^0}{\hat{\rho}^R}, u_x{}^0 = \frac{\hat{u}_x{}^0}{\sqrt{\hat{R}^R \hat{T}^R}}, u_y{}^0 = \frac{\hat{u}_y{}^0}{\sqrt{\hat{R}^R \hat{T}^R}}, R^0T^0 = \frac{\hat{R}^0 \hat{T}^0}{\hat{R}^R \hat{T}^R}, p^0 = \frac{\hat{p}^0}{\hat{\rho}^R \hat{R}^R \hat{T}^R}.
\end{aligned} \tag{6.6}
$$

A little modification has been done to the LBM model to make it suitable for multi-fluid flows. The variable T has been replaced by the term RT in the equations 4.11 – 4.22. This modification makes the LBM model suitable for multi fluid-flows and it can now be used to calculate inter-cell parameters from the node parameters.

The solution procedure with the hybrid model has been explained in a stepwise manner in the chapter 5. The new hybrid method has been benchmarked for the multi-fluid flows using the shock tube problem. Again, the computational time has been significantly reduced by the FVM–LBM method. The method is also able to accurately simulate the shock profile. A robust computational solver has been developed using the new hybrid FVM–LBM method which is accurate and computationally efficient.

Chapter 7

Results

The LBM model (proposed by Kataoka and Tsutahara), and the new LBM scheme have been benchmarked for several test cases. The test descriptions are given below:

a. Shock tube problem (1D): The gases in the two sections are separated by a diaphragm. When the diaphragm is broken, a shock wave propagates in one of the sections and an expansion wave propagates in the other. The initial parameters on left and right sides of the diaphragm are,

$(\rho_L , u_L, T_L \ = \ 1, 0, 1)$ $\qquad$ $x < 0$

$(\rho_R , u_R, T_R = \ 5, 0, 1)$ $\qquad$ $x > 0.$

b. Shock Expansion in open space (2D): This test [19] is used to benchmark the new FVM-LBM method for 2D inviscid Euler problems. The initial and boundary conditions have been indicated in the figure 4.

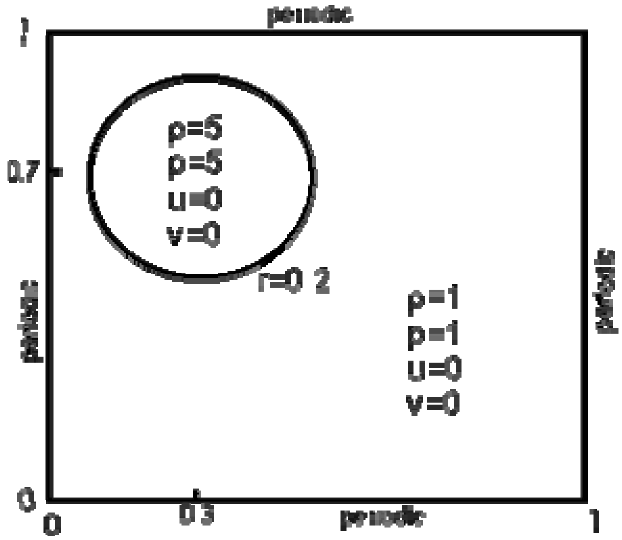

Fig 4: Shock expansion in open space – Initial and Boundary Conditions

c. Riemann Problem: The fundamental difference between a shock tube problem and Riemann problem is that the velocity in the two sections for a Riemann problem is not zero. This problem consists of initial flow parameters on left and right sides separated by a discontinuity. Riemann problem generates flow with steep variations. It is the elementary problem which is solved in all inviscid Euler schemes to obtain the cell inter-cell parameters from cell node parameters. The initial value problem is:

   (ρ_L , u_L, T_L = 1, 1, 1) $x < 0$

   (ρ_R , u_R, T_R = 1, -1, 1) $x > 0$.

d. Roe Test: Expansion fans are generated on both sides of the diaphragm. This problem consists of the following initial flow parameters on left and right sides,

   (ρ_L, u_L, T_L = 1, -1, 1.8) $x < 0$

   (ρ_R , u_R, T_R = 1, 1, 1.8) $x > 0$.

7.1 Results from the conventional LBM model

Initially, the conventional Lattice Boltzmann model was used to simulate the shock tube problem. This model could simulate shock tube problem for relatively small initial pressure ratios only. The conventional LBM models fluid as consisting of particles which perform the successive processes of collision and propagation. Severe oscillations were observed with this LBM model in the profiles of parameters (velocity, pressure, density and temperature). The limitations of the model for incompressible flows provided a motivation to study LBM models for compressible flows.

The results obtained by the conventional model for the shock tube problem with an initial pressure ratio equal to 3 have been shown in the figure 5. The three waves i.e. shock wave (at X = 0.75), contact discontinuity wave (at X = 0.32) and expansion fan (*Head* at X = 0.60 and *Tail* at X = 0.30) can be observed in the pressure and temperature profiles (Figure 5(a), 5(b)). The pressure and temperature ratios across the shock wave are 1.73 and 1.76 respectively. The magnitude of oscillations is significantly large near the discontinuity region, so alternative compressible flow models have to be studied.

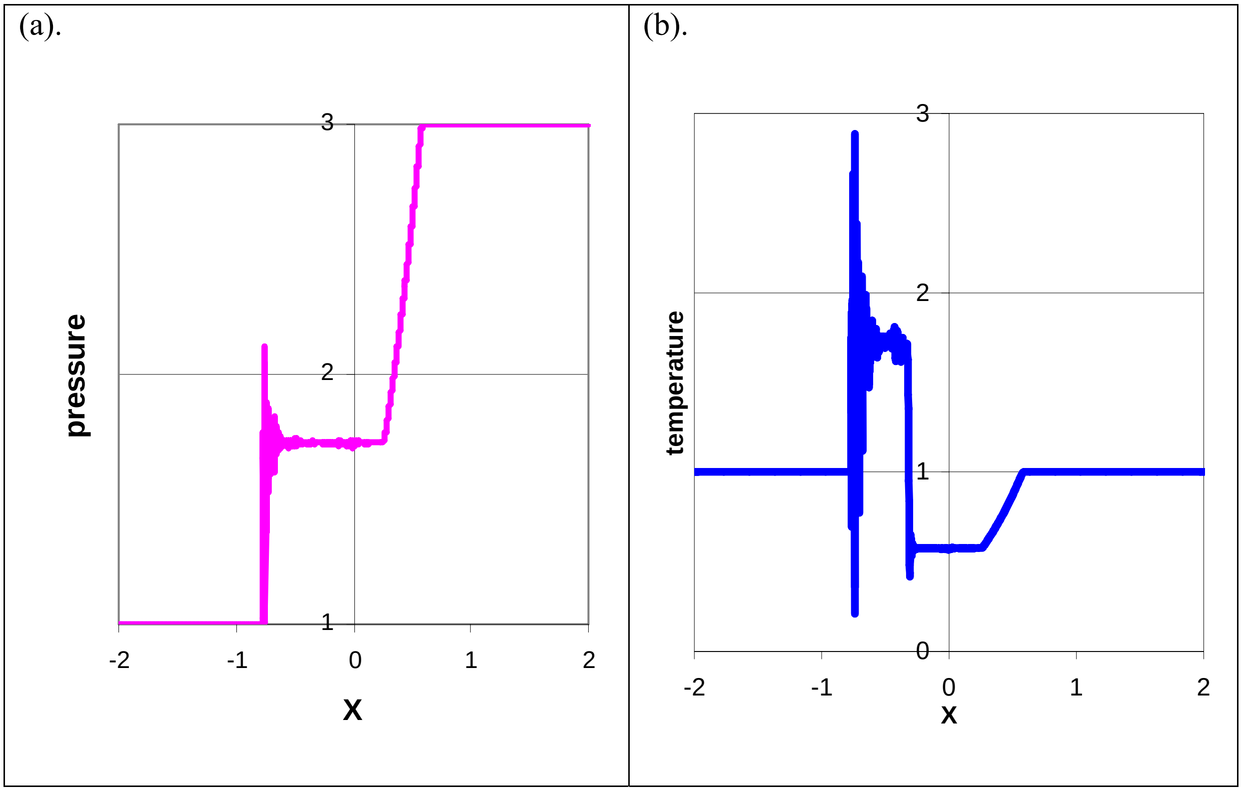

Fig 5: Shock tube problem results with incompressible LBM at time t = 1 (Δx = .001)
(a). Pressure (b). Temperature

7.2 Results from LBM (Kataoka and Tsutahara) Model

CFD results for shock tube problem, Riemann problem and Roe Test have been obtained by LBM simulation. All these results show an exact matching with the analytical solutions of these problems. But the limitation of this approach is that some severe oscillations are observed at shock and contact discontinuity regions when higher order schemes are used. Dissipation is significantly high with lower order schemes. The oscillations upon interaction with other waves generate a chaotic profile for the macroscopic parameters (with random oscillations) which is undesirable. The oscillations are found to be dependent upon Knudsen number (ε) (see Eq. 4.15). Lower Knudsen number generates steep shock profile but the simulation time and severity of oscillation increases.

a. Shock tube problem

Shock Tube problem is a standard benchmarking test for all the compressible inviscid flows as it includes all the three elementary waves that may be present in a compressible fluid flow problem: shock wave, contact discontinuity and expansion fan wave. The steep shock wave (at X=-1.7) propagating towards left and expansion fan (*Head* at X=1.2 and *Tail* at X=0.4) propagating towards the right can be observed in the macroscopic parameter profiles which are shown in figure 6. A contact discontinuity wave (at X=-0.7) propagating towards left is also observed in density and temperature profiles.

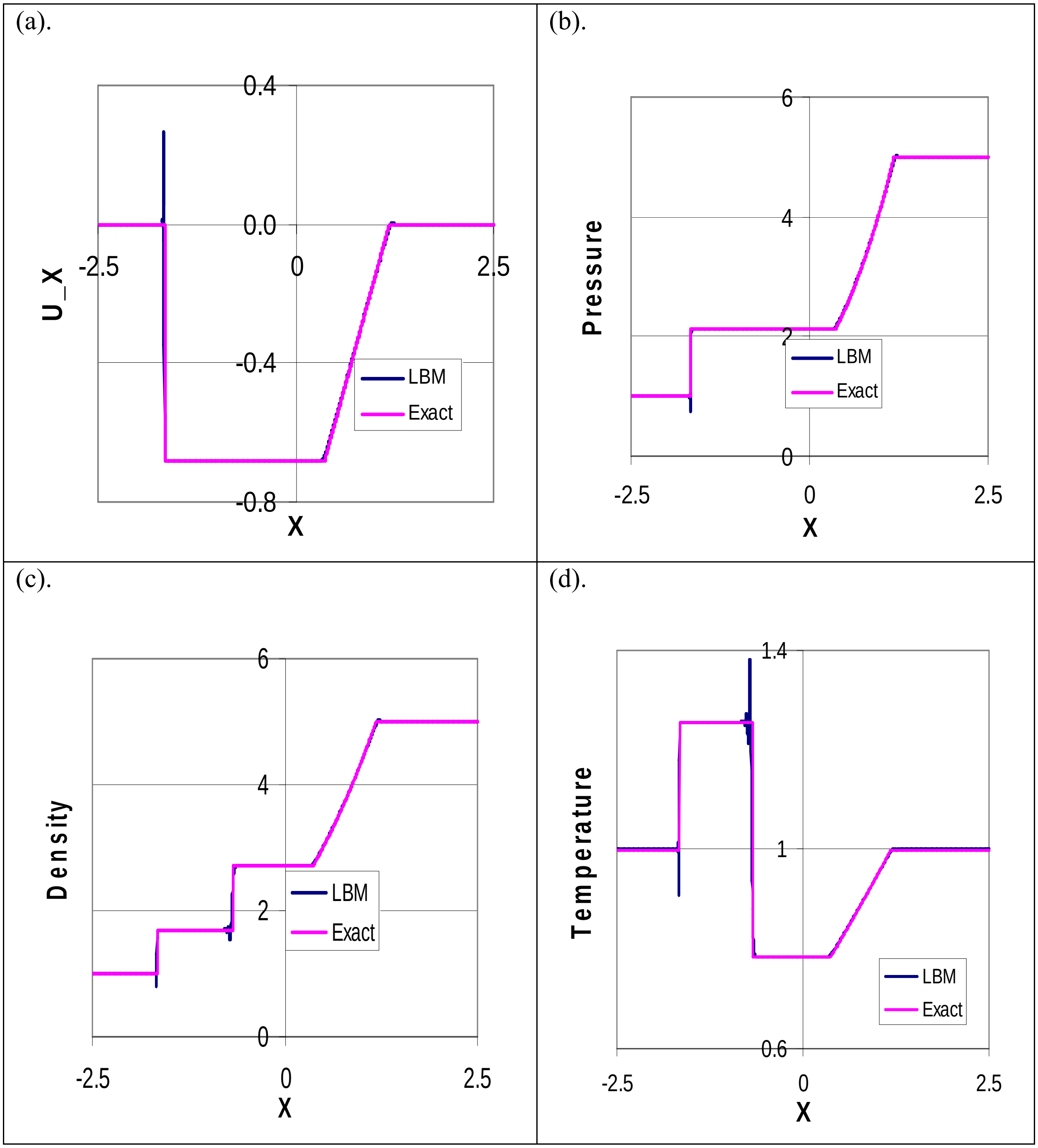

Fig 6: LBM results for shock tube problem after time t = 1 (Δx = .002, ε = .0001, γ = 1.4)
(a). Velocity (b). Pressure (c). Density (d). Temperature

As discussed earlier, some oscillations are observed with the numerical method by Kataoka and Tsutahara with second order discretization in space. A total of 2500 node points have been used for these simulations. If the number of node points is reduced (or if the Knudsen number is increased), then the computation time reduces considerably as well as the severity of the oscillations decreases. But a reduction in the number of node points makes the shock profile less steep.

b. Riemann problem

The solution to Riemann problem is the basic step in obtaining the results with FVM and with the new hybrid FVM–LBM method. Local Riemann problems are solved by Godunov scheme in the FVM and by LBM in the hybrid method. The solution of Riemann problem obtained by LBM using second order discretization in space and the results are shown in figure 7. Two shock waves (at X = 0.95 and at X = -0.95), which are propagating on the either side of initial discontinuity, can be seen in the solution profiles of the macroscopic parameters. Another feature of this Riemann problem is that contact discontinuity wave is absent. Severe oscillations are again present at the location of discontinuities. The severity of oscillations can be reduced by using smaller number of node points, but that will affect the simulation accuracy of shock waves.

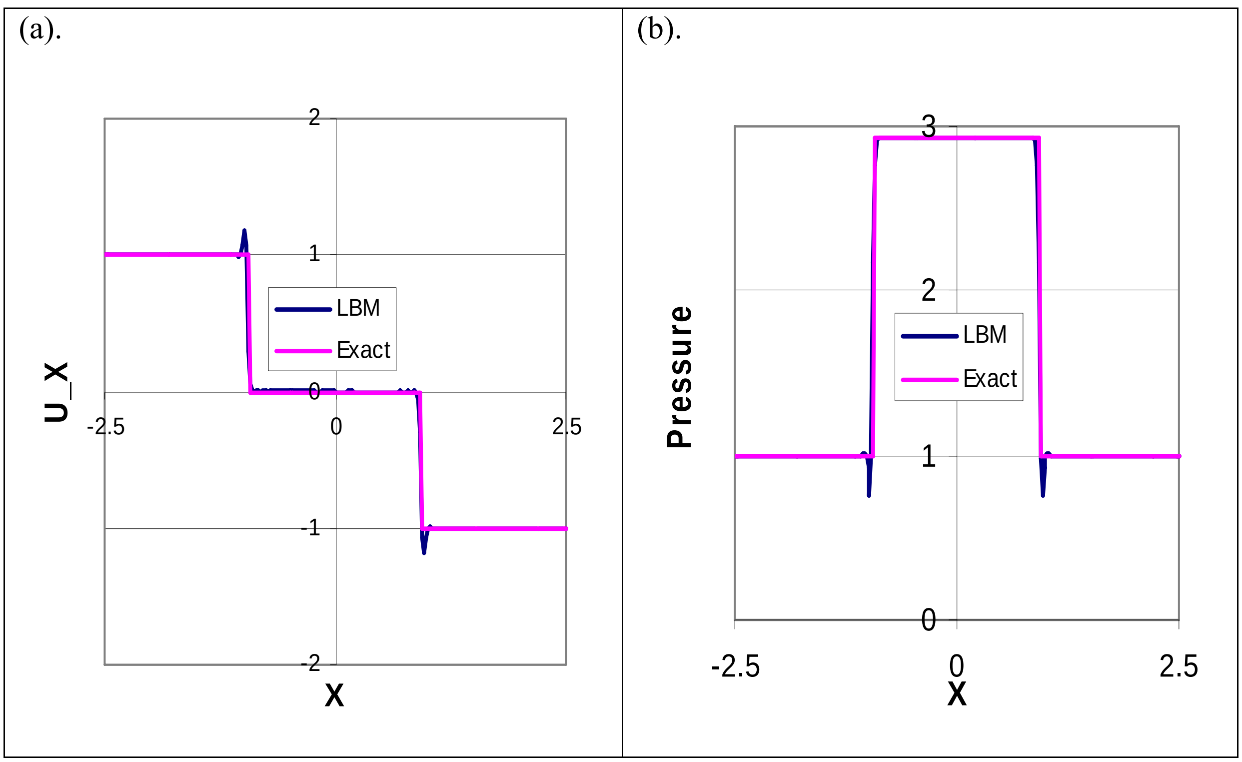

(c). (d).

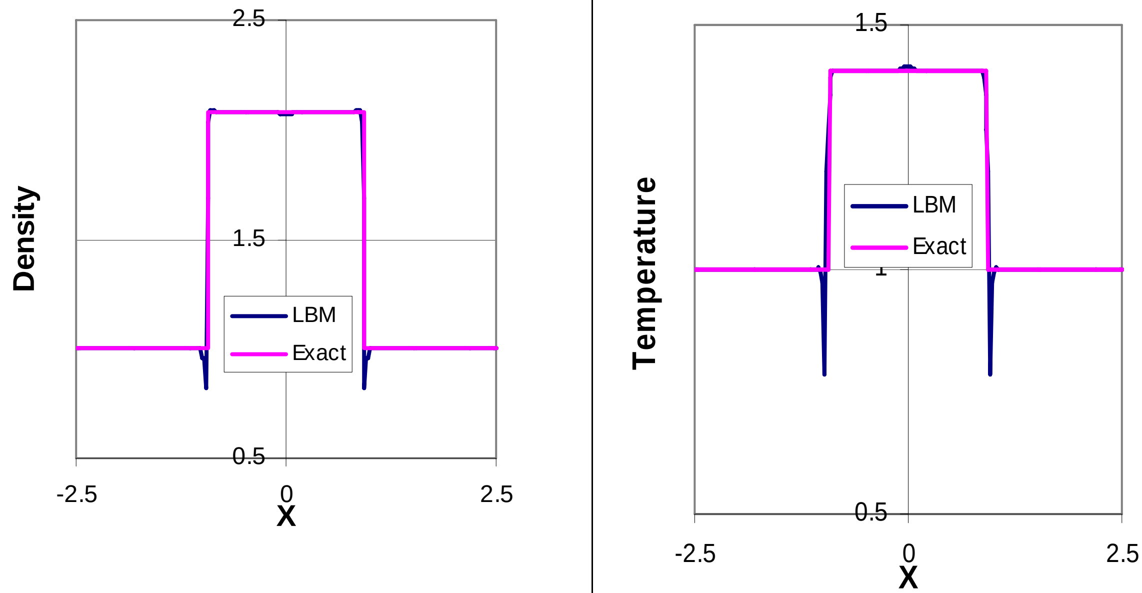

Fig 7: LBM results for Riemann problem after time t = 1 ($\Delta x = .02$, $\varepsilon = .001$, $\gamma = 1.4$)
(a). Velocity (b). Pressure (c). Density (d). Temperature

c. Roe test

This is another test case which has been used to benchmark the compressible LBM model by Kataoka and Tsutahara for one-dimensional problems. The flow is moving away from the initial discontinuity in the Roe test whereas the flow was moving towards the initial discontinuity in the case of Riemann problem and this generates a wave structure which is different from the one which was generated in the case of Riemann problem. The results obtained for the Roe Test have been shown in the figure 8.

Two expansion fans move on the either side of initial discontinuity. The right moving expansion fan has its *Head* at X = 2.5 and *Tail* at X = 1.3, while the left moving expansion fan has its *Head* at X = -2.5 and *Tail* at X = - 1.3. Similar to the case of the earlier Riemann problem, the contact discontinuity wave is also absent in the Roe Test. Small oscillations were observed near the initial discontinuity. These oscillations have been also observed in some high resolution schemes and the reason in supposed to be an inappropriate choice of the time step and the Knudsen number [13].

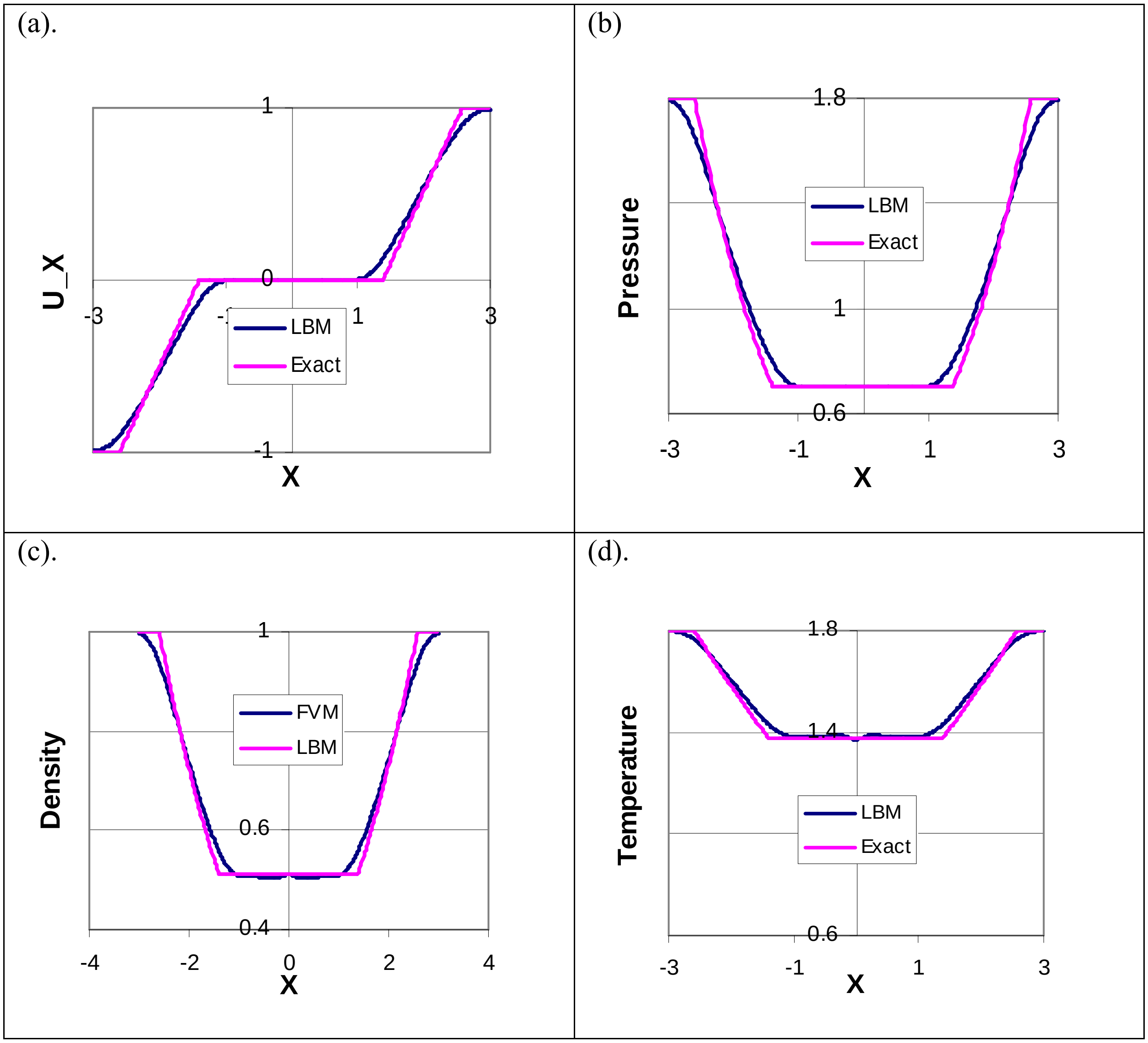

Fig 8: LBM results for Roe test after time t = 1 ($\Delta x = .02$, $\varepsilon = .001$, $\gamma = 1.4$). (a) Velocity (b). Pressure (c). Density (d). Temperature

7.3 Results from the new hybrid FVM - LBM method

The new hybrid FVM - LBM method (denoted by FVM+LBM) is computationally more efficient as compared to the conventional FVM along with the use of Godunov scheme. The results obtained with the new method have been compared with the results from FVM and the exact analytical solution. The comparisons have been shown in this section for several benchmarking test cases and it can be observed that the new method is capable of simulating sharp shock and contact discontinuity waves. The method has been benchmarked by shock tube problem (1-D), shock expansion problem (2-D), Roe Test and Riemann problem.

a. Shock tube problem

The new method simulates a steep shock and contact discontinuity profile as compared to the profile obtained by FVM along with the use of Godunov scheme to calculate the inter-cell parameters. A comparison of the results by the new method for the shock tube problem with the exact solution and with FVM has been shown in figure 9. The accuracy in simulation of discontinuity waves (shock and contact discontinuity) is evident from the comparisons. The new method is computationally efficient and requires a significantly less computation time (33.6 s) as compared to the computation time of FVM along with Godunov scheme (45.7 s), that is an improvement by about 24% in computational time..

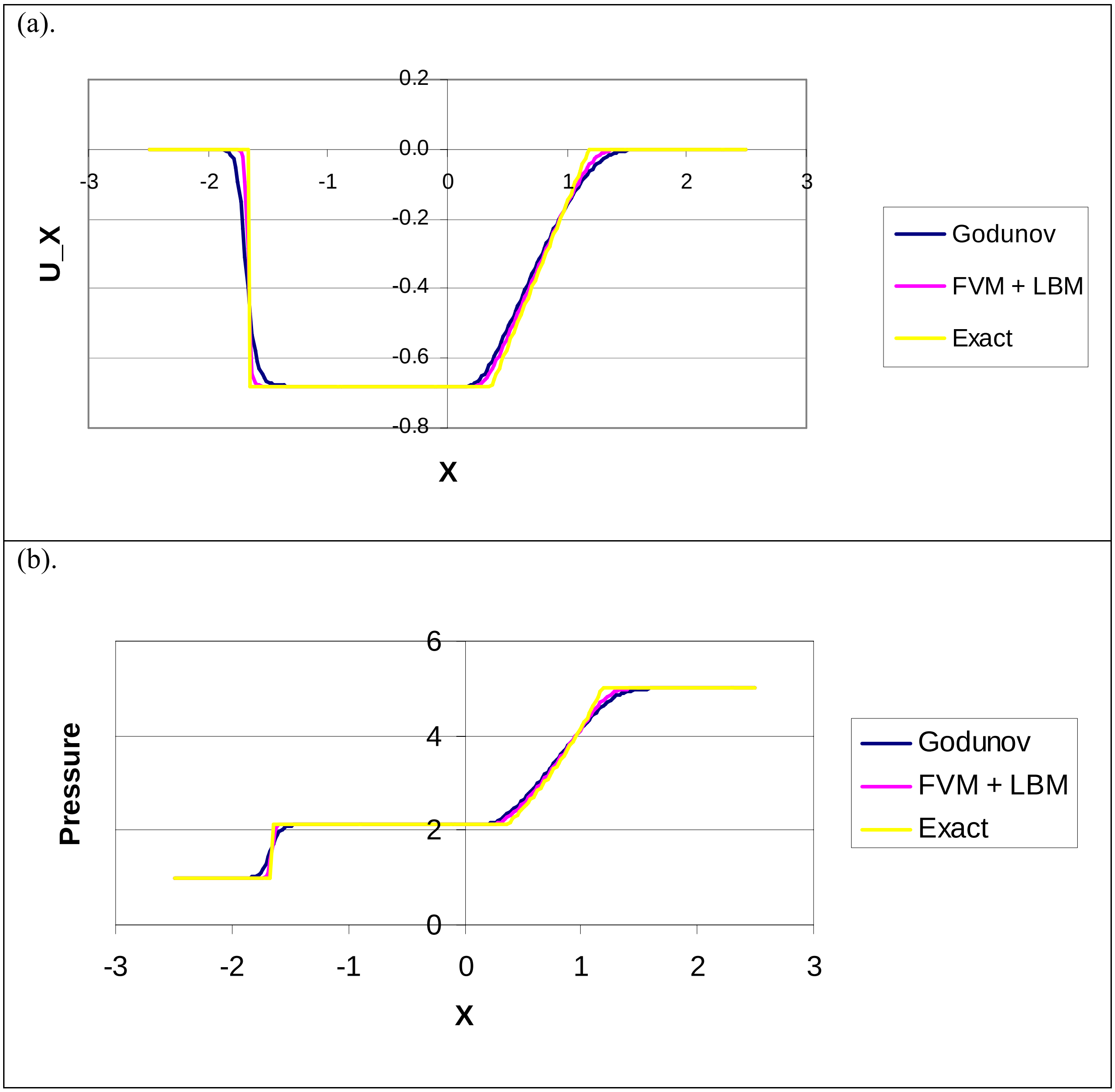

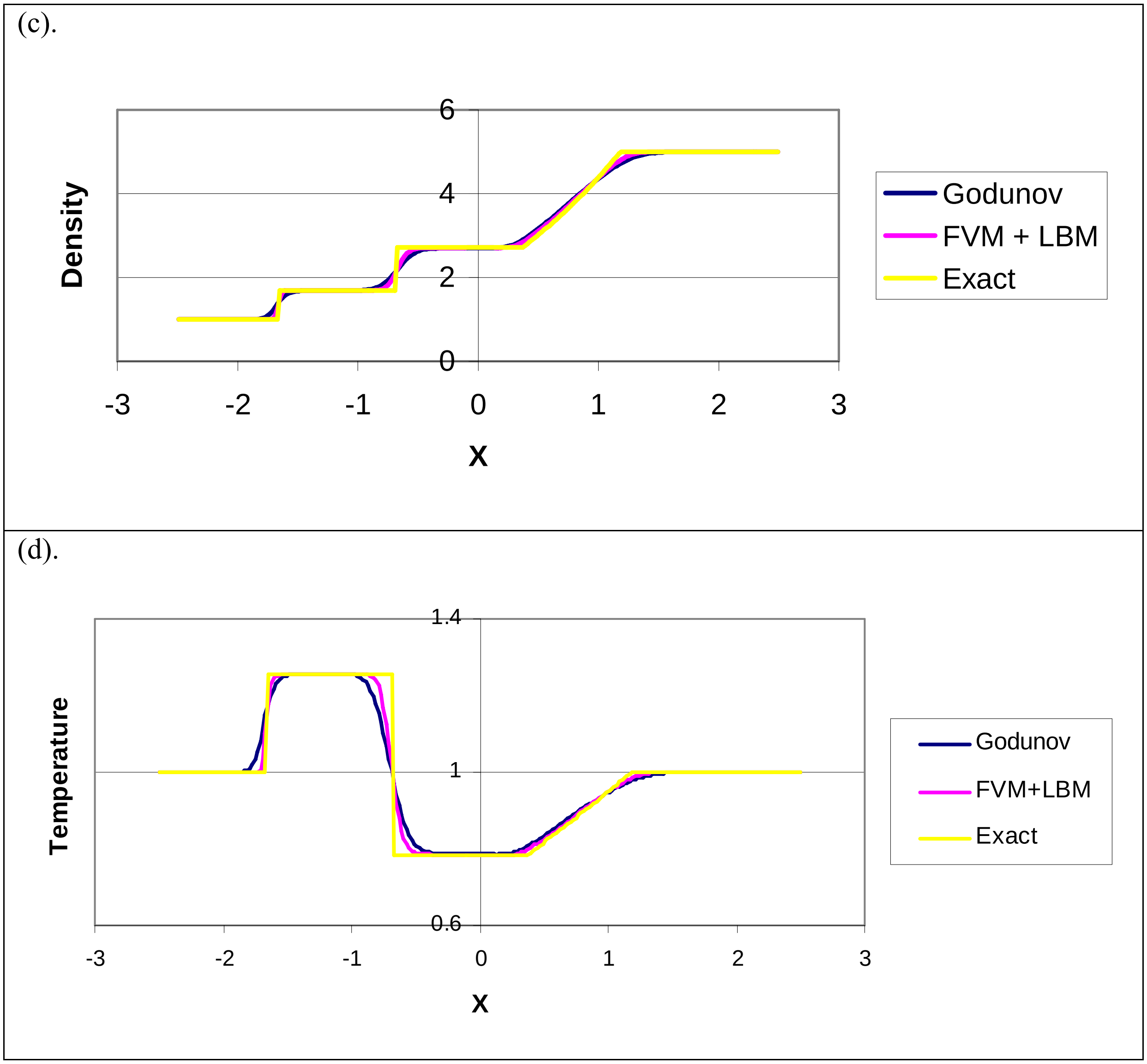

Fig 9: Results for Shock Tube problem after time t = 1 ($\Delta x = .02$, $\varepsilon = .001$, $\gamma = 1.4$)
(a). Velocity (b). Pressure (c). Density (d). Temperature

All the three waves (shock wave, contact discontinuity wave and expansion fan) have been accurately simulated by the new method. The jumps across the shock wave in pressure, density and temperature are 2.13, 1.69 and 1.29 (Figures 9(b), 9(c), 9(d)) respectively. The contact discontinuity wave moves at a speed of 0.68 towards the left of initial discontinuity which is equal to the velocity drop across the shock wave (Figure 9(a)). The temperature drops from 1.29 to 0.79 (Figure 9(d)) and density increases from 1.69 to 2.72 (Figure 9(c)) across the contact discontinuity. The new method simulates more accurate shock wave (at X = -1.7), contact discontinuity wave (at X = -0.7) and expansion fan (*Head* at X = 1.2 and *Tail* at X = 0.4) as compared to the results obtained by FVM along with the Godunov scheme.

b. Riemann problem

Local Riemann problems have to be analytically solved in each time step of the Godunov scheme. The LBM by Kataoka and Tsutahara is used to simulate the Riemann problem in the hybrid FVM–LBM method and the results match analytically. The wave structure of Riemann problem consists of two shock waves which move on the either side of initial discontinuity. The contact discontinuity wave is absent in this Riemann problem. Once again, the new method is computationally efficient and requires a significantly less computation time (34.8 s) as compared to the computation time of FVM along with the use of Godunov scheme (46.4 s) to compute inter-cell parameters, which is an improvement by about 25% in computational time.

(a).

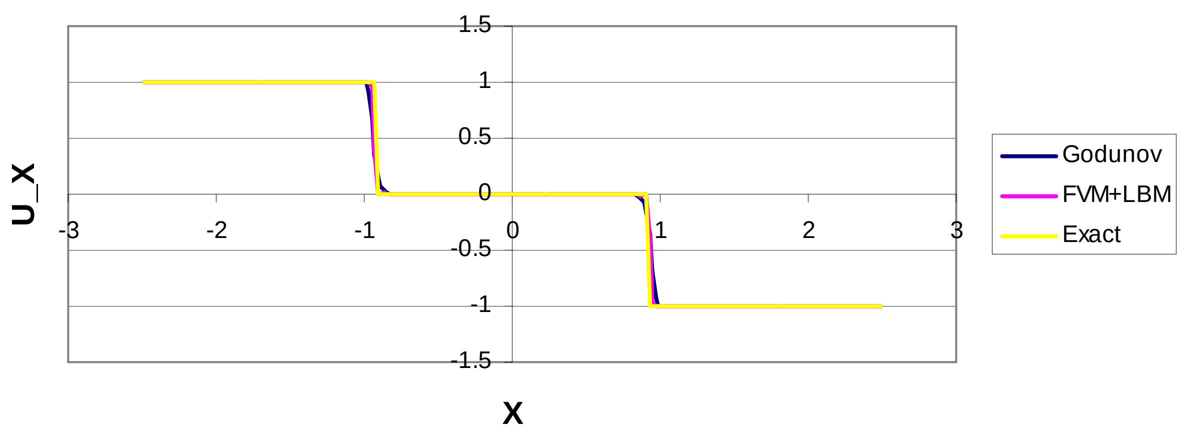

(b).

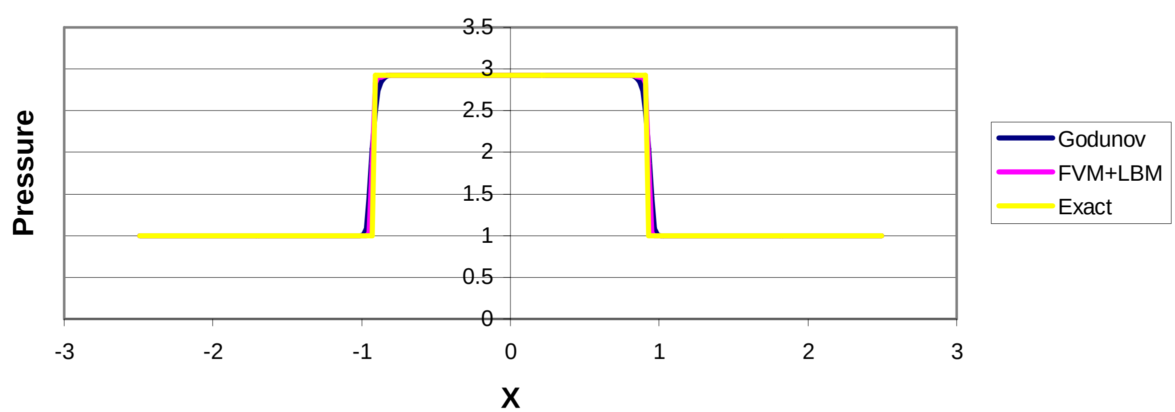

(c).

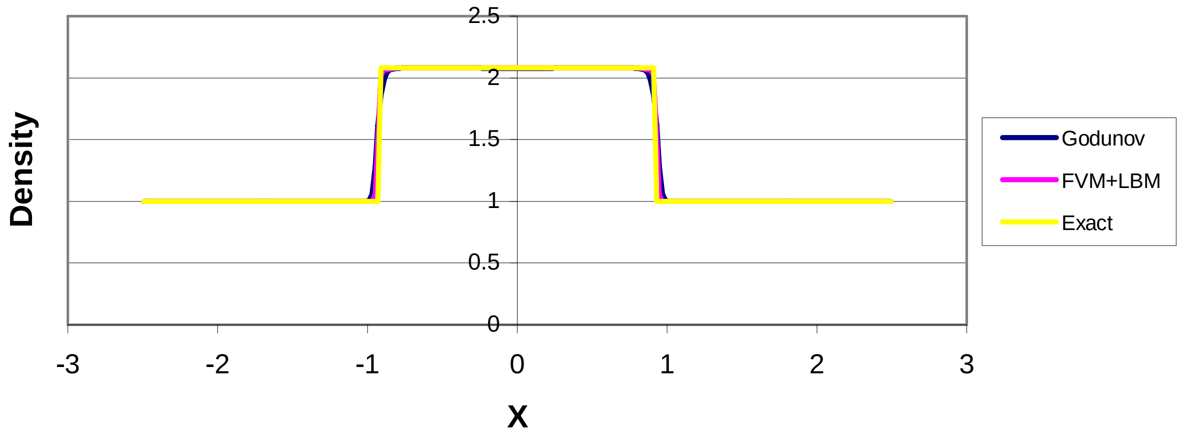

(d).

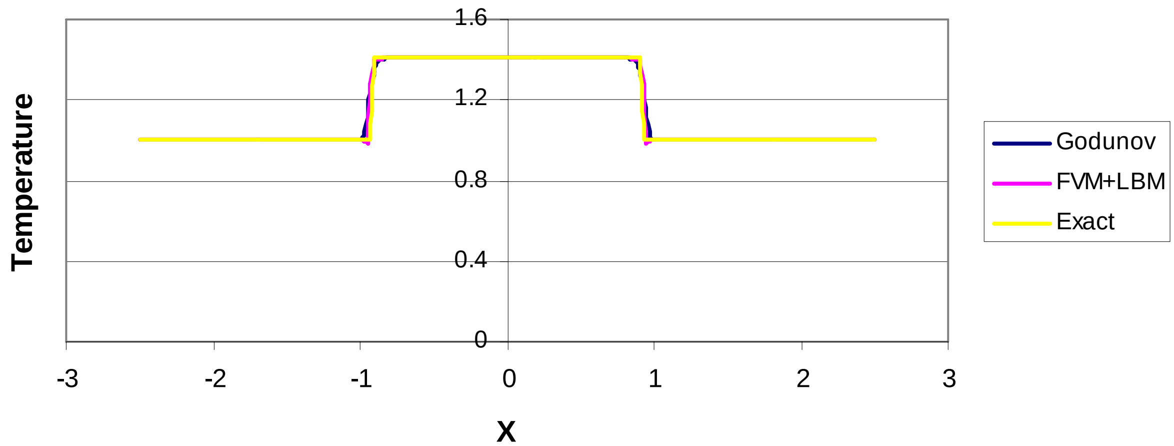

Fig 10: Results for Riemann problem after time t=1 ($\Delta x = .02$; $\varepsilon=.001$, $\gamma = 1.4$)
(a). Velocity (b). Pressure (c). Density (d). Temperature

The new FVM – LBM method simulates accurate shock profiles for the Riemann problem which is evident from the results shown in figure 10. The jumps across the shock wave in pressure, density and temperature are 2.93, 2.08 and 1.41 respectively (Figure 10(b), 10(c), 10(d)). The flow in between the shock waves is stationary (Figure 10(a)). The comparisons between the FVM along with Godunov scheme, new FVM – LBM method and the exact solution shows that the new method accurately simulates the two shock waves (at X = 0.95 and at X = -0.95) on the either side of initial discontinuity.

c. Roe test

The new FVM – LBM method has also been benchmarked by the Roe test. Contrary to the wave structure of Riemann problem which was described earlier, the solution of Roe test consists of two expansion fans which move on the either side of initial discontinuity. Again, the contact discontinuity wave is absent in the Roe Test. It has again been observed that the new method is computationally efficient and requires a significantly less computation time (7.19 s) as compared to the computation time of FVM along with the use of Godunov scheme (8.50s) to compute inter-cell parameters. The computational time required by the new method is about 16% less than the time required by pure FVM. The new FVM – LBM method simulates accurate wave profiles for the Roe test which is evident from the results shown in figure 11.

(a).

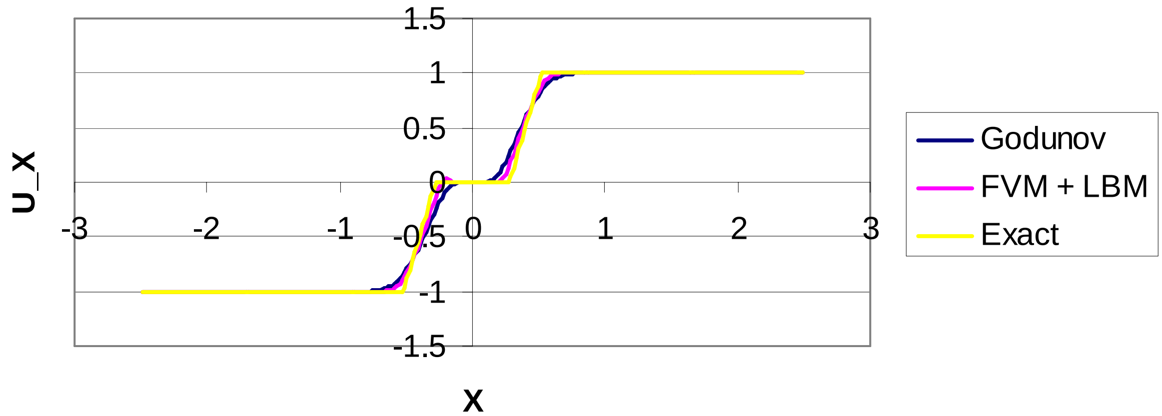

(b).

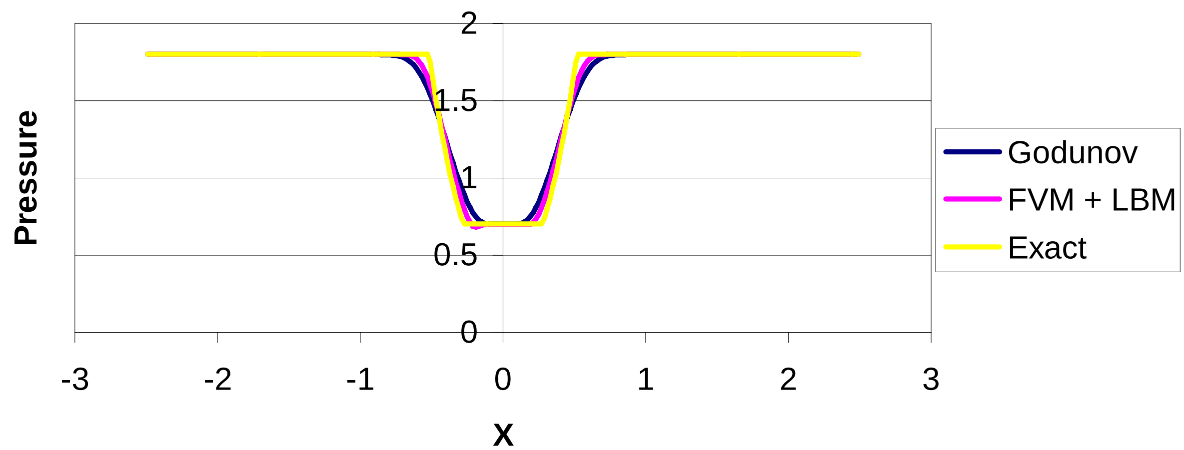

(c).

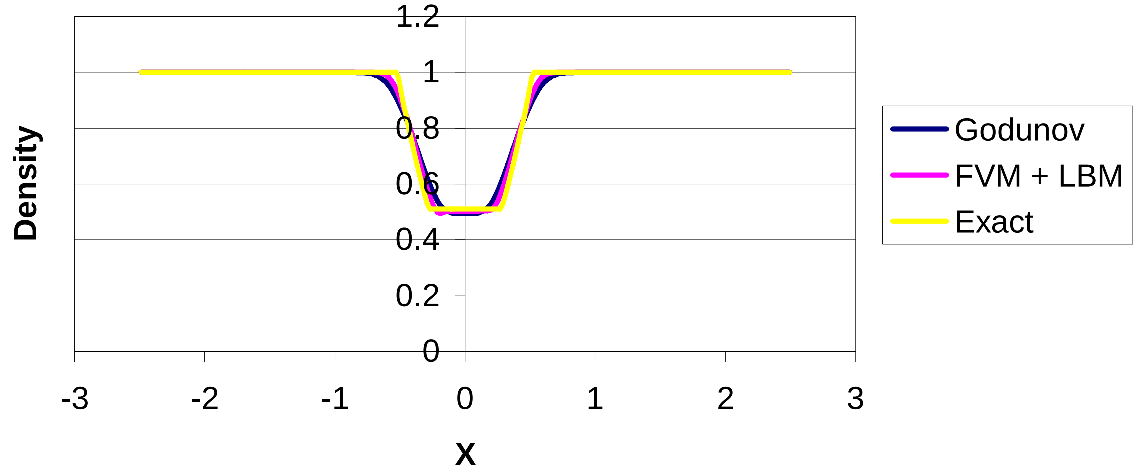

(d).

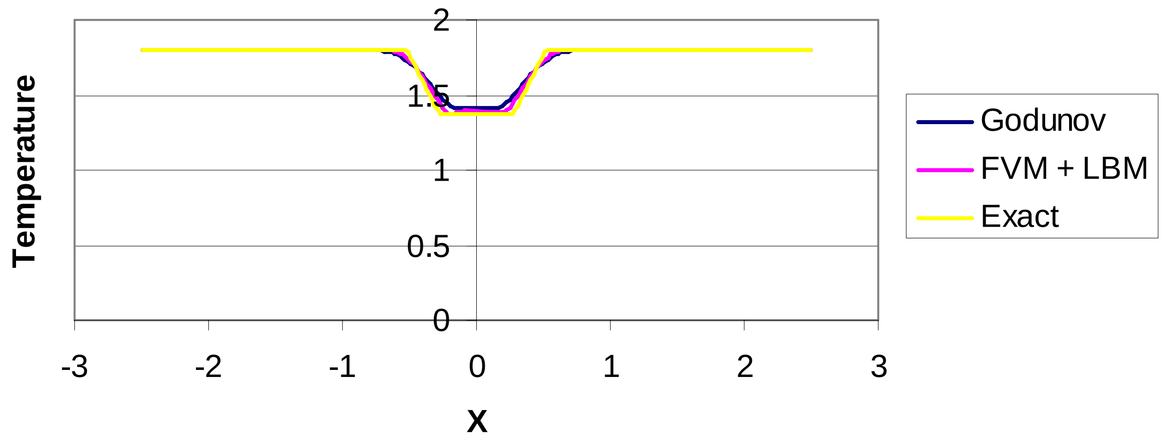

Fig 11: Results for Roe Test after time t = 0.2 (Δx = .02; ε = .001, γ = 1.4)
(a). Velocity (b). Pressure (c). Density (d). Temperature

The results show that pressure drops from 1.80 to 0.70 (Figure 11(b)), density drops from 1.00 to 0.51 (Figure 11(c)) and temperature drops from 1.80 to 1.38 (Figure 11(d)) across the expansion fan. The flow in between the expansion fan waves is stationary (Figure 11(a)). The comparisons between the FVM along with Godunov scheme, new FVM – LBM method and the exact solution shows that the new method accurately simulates the two expansion fan waves (*Head* at X= 0.54, *Tail* at X=0.30 and *Head* at X= -0.54, *Tail* at X=-0.30) on the either side of initial discontinuity.

d. Shock expansion problem in a 2-D open space

Circular shock-waves expand and interact in open space. This test case [19] demonstrates that the new scheme can effectively handle 2-D flows and multiple periodic boundary conditions correctly. The pressure contour plot of the problem obtained from its source website [19] is given in figure 12. Results obtained after time t=0.84 are also shown in form of contour and vector plots.

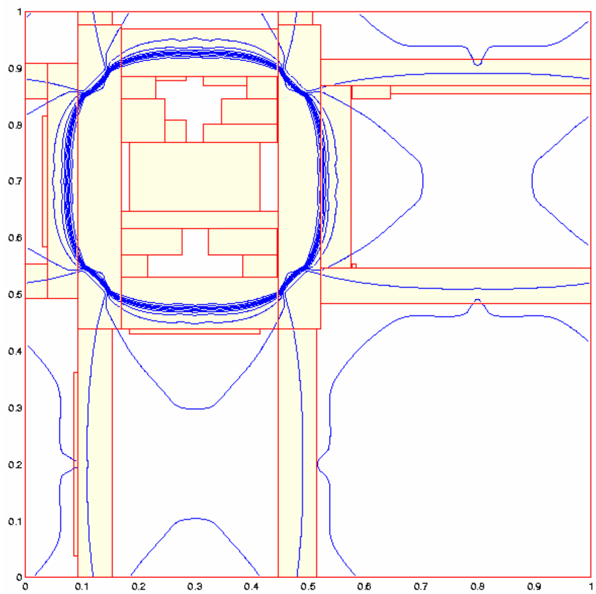

Fig 12: Pressure contour plot from source [19] for 2-D shock expansion problem

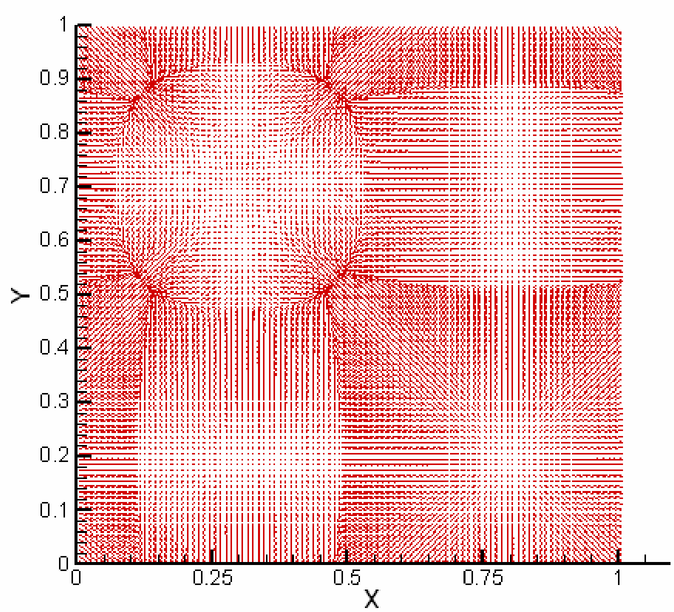

Fig 13: Velocity vector plot for 2-D shock expansion problem in an open space

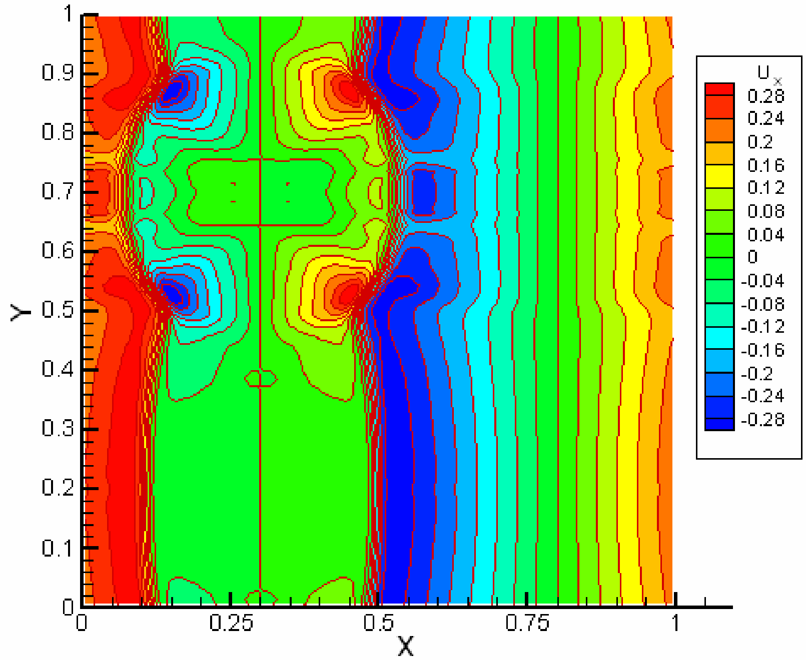

Fig 14: x-velocity contour map for 2-D shock expansion problem in an open space

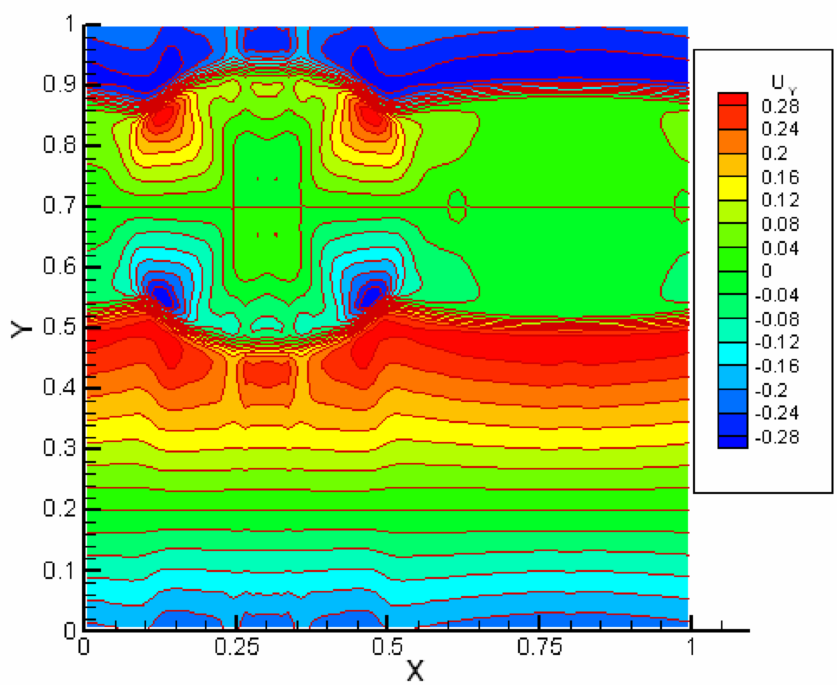

Fig 15: y-velocity contour map for 2-D shock expansion problem in an open space

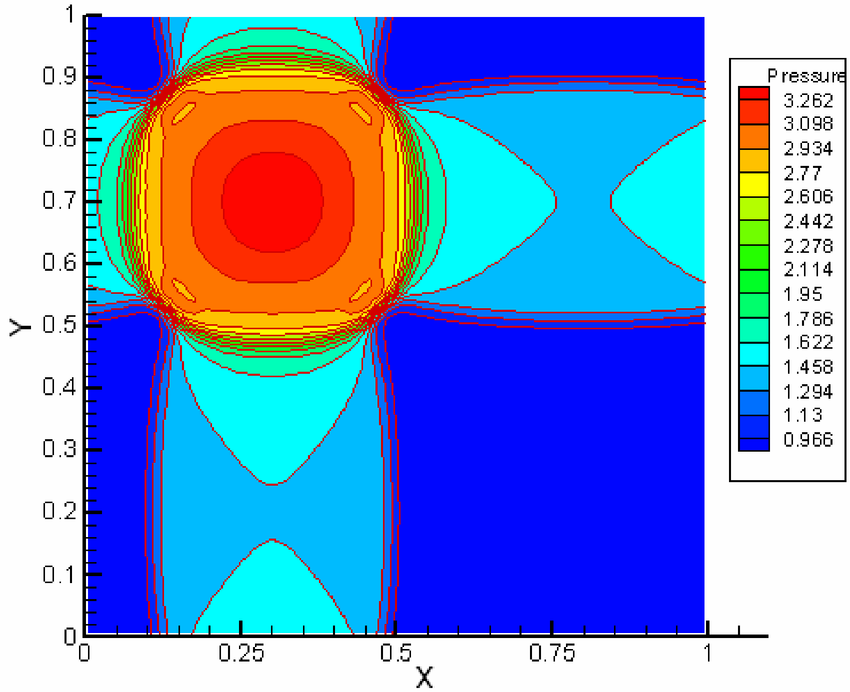

Fig 16: Pressure contour map for 2-D shock expansion problem in an open space

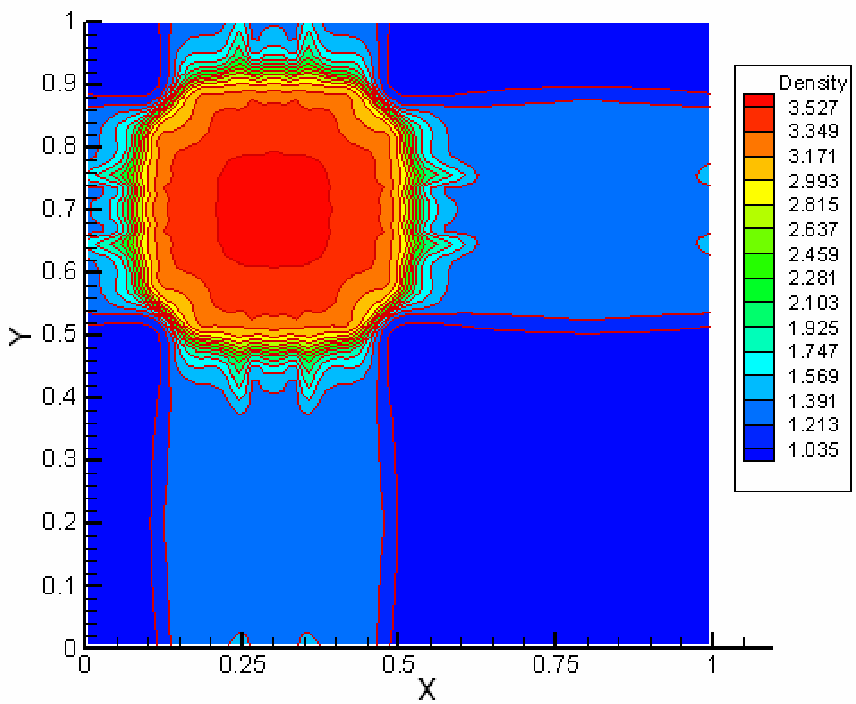

Fig 17: Density velocity contour map for 2-D shock expansion problem in an open space

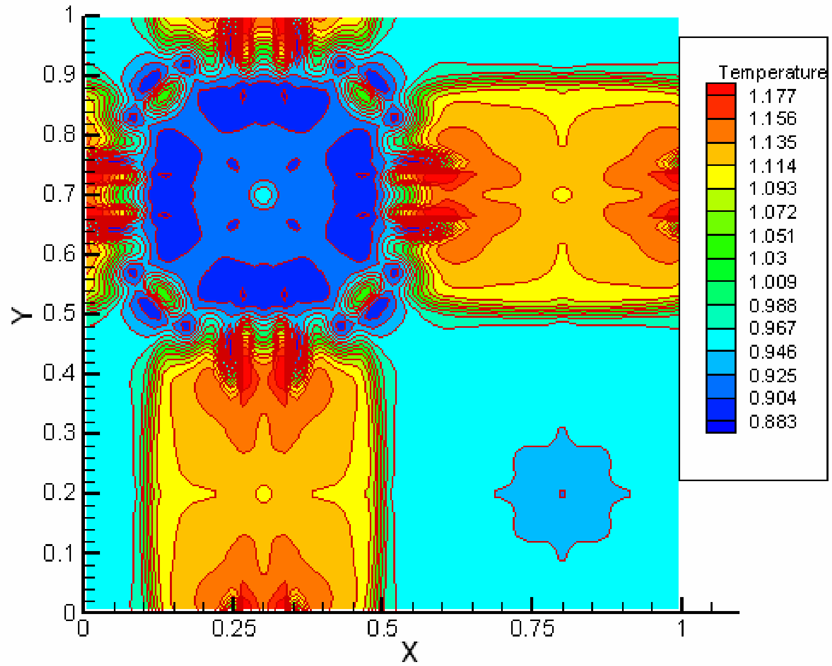

Fig 18: Temperature contour map for 2-D shock expansion problem in an open space

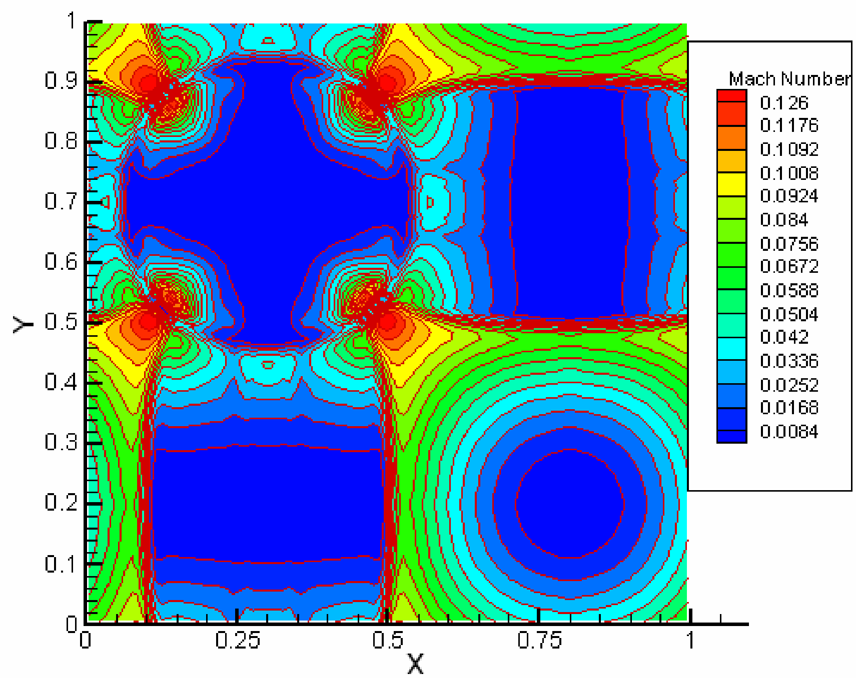

Fig 19: mach number contour map for 2-D shock expansion problem in an open space

This is the first test which has benchmarked the method for 2-D flows. The pressure contour has been compared with the pressure contour obtained from the website (Figure 12) [19] which was the source of this problem. It is indeed interesting to note the symmetry of pressure, temperature, density and Mach number contours across the diagonal line which is due to the presence of symmetry boundary conditions. Effects of expanding circular shock and its interaction with the surrounding space upon the macroscopic parameters can be observed from the velocity vector plot (figure 13), velocity contour plots (figure 14 and figure 15), pressure contour pot (figure 16), density contour plot (figure 17), temperature contour plot (figure 18) and Mach number contour plot (figure 19).

A comparison between the results obtained from the FVM (along with Godunov scheme), the proposed FVM-LBM hybrid method and the exact solution for the shock tube problem, Riemann problem and Roe test has been made in the above section. The results show that the new scheme gives higher accuracy in comparison to the FVM. It has also been observed that the new scheme is computationally more efficient (reduces CPU processing time by around 22%). The new scheme thus incorporates the advantages of both FVM and LBM.

7.4 Results from the model (by Wang et al.) for multi-fluid flows

The multi-fluid flow model proposed by Wang et al. [15] involves two new formulations for determining the ratio of specific heats of the mixture and the molecular weight of the mixture in addition to the Euler equations. This model has been benchmarked for different test cases which have been used as benchmarking cases in the publication by Wang et al.. The results obtained using this model along with the first-order Godunov scheme are shown and discussed below.

Case 1: A shock tube initially filled with two different gases is considered. Two initial constant states are defined as

$(\rho_L, u_L, p_L, \gamma_L, C_{vL} = 14.54903, 0.0, 19430000, 1.67, 2420)$ $\quad x < 0.5$

$(\rho_R, u_R, p_R, \gamma_R, C_{vR} = 1.16355, 0.0, 100000, 1.4, 732)$ $\quad x > 0.5$

The results obtained by the multi-fluid model have been shown in figure 20. All the three elementary waves i.e. the shock wave, the contact discontinuity wave and the rarefaction wave are present in the solution to the shock tube problem.

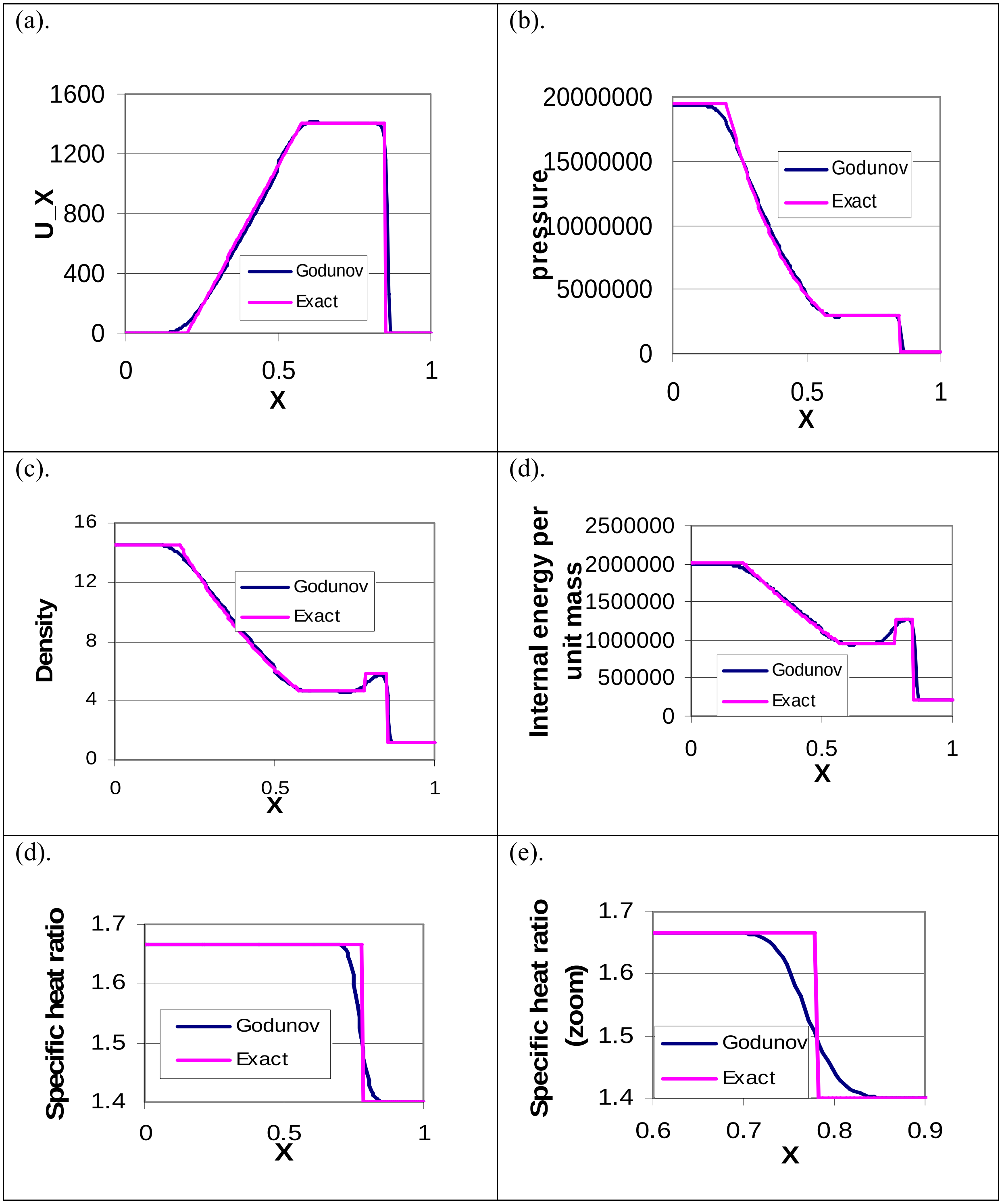

Fig 20: Results for Case 1 after time t = 200 μs (Δx = .005). (a). Velocity (b). Pressure (c). Density (d). Temperature (e). specific heat ratio (f). zoomed specific heat ratio

The shock wave (at X = 0.85), the contact discontinuity wave (at X = 0.78) (Figure 20(e) and Figure 20(f)) and the rarefaction wave (*Head* at X = 0.20 and *Tail* at X = 0.60) have been accurately simulated by the multi-fluid model proposed by Wang et al.. Across the shock wave, velocity jumps from 1400 m/s to 0 m/s (Figure 20(a)), pressure jumps from 3000000 N/m^2 to 100000 N/m^2 (Figure 20(b)), density jumps from 6 Kg/m^3 to 1.16355 Kg/m^3 (Figure 20(c)) and the internal energy per unit mass jumps from 1250000 J/Kg to 210000 J/ Kg (Figure 20(d)). The velocity in the region between the expansion fan wave and the shock wave is equal to 1400 m/s. These results compare well with the exact solution. Note that these quantities are being reported in their dimensional form.

Significantly large numerical diffusion has been observed and second-order Godunov scheme is often used to improve the accuracy of the results. This model gives much accurate results for specific heat ratio in comparison to the results obtained from some of the conventional numerical models for multi-fluid flows.

Case 2: This test case consists of a shock tube filled with air, where a shock wave moves to the right. In the pre-shock state, a slab of helium is located between x = 0.4 m and x = 0.6 m. The shock wave is initially located at x = 0.25 m. The initial conditions and properties are given as

$(\rho, u, p, \gamma, C_v = 1.3765, 0.3948, 1.57, 1.40, 0.72)$ $\quad 0.00 < x < 0.25$

$(\rho, u, p_, \gamma, C_v = 1.0000, 0.0000, 1.00, 1.40, 0.72)$ $\quad 0.25 < x < 0.40$

$(\rho, u, p_, \gamma, C_v = 0.1380, 0.0000, 1.00, 1.67, 2.42)$ $\quad 0.40 < x < 0.60$

$(\rho, u, p_, \gamma, C_v = 1.0000, 0.0000, 1.00, 1.40, 0.72)$ $\quad 0.60 < x < 1.00$

The results obtained by the multi-fluid model for the case 2 have been shown in figure 21.

(a). (b).

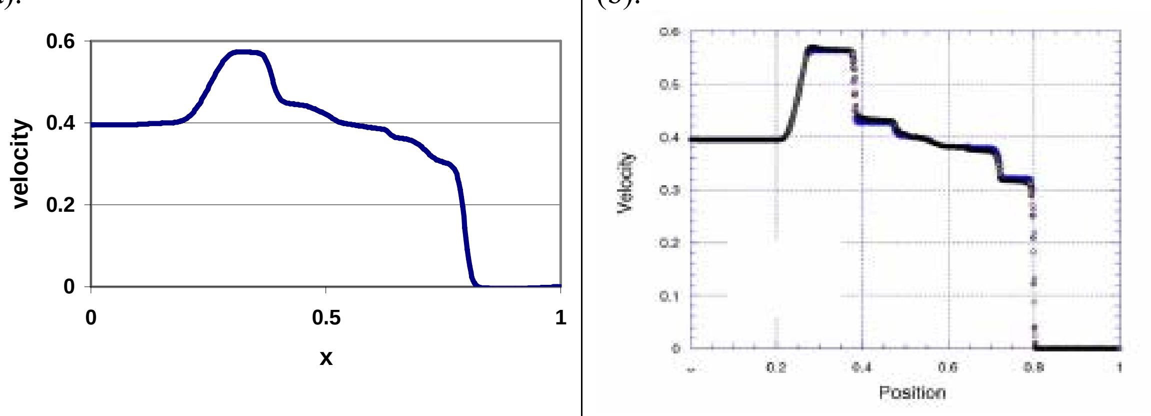

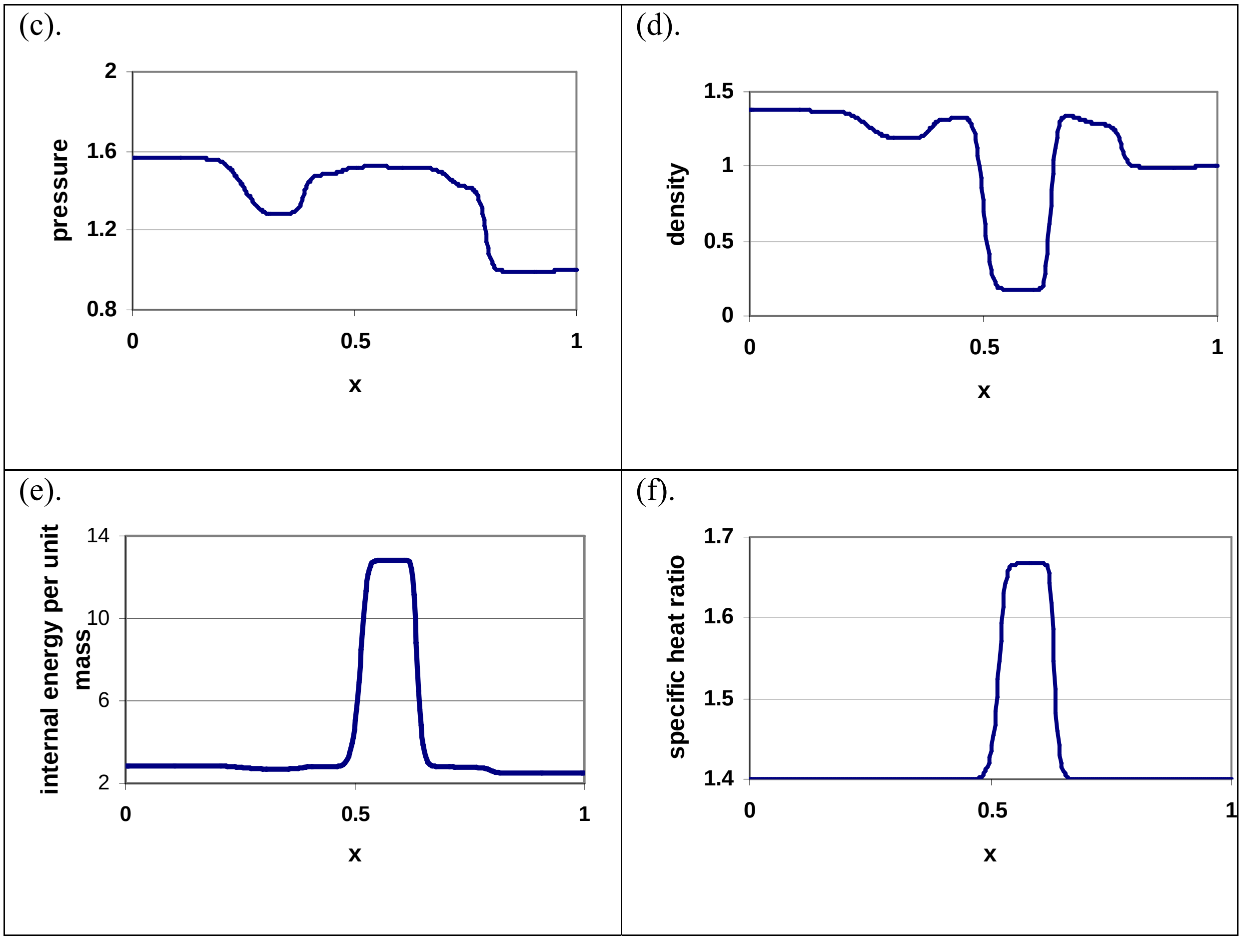

Fig 21: Results for Case 2 after time t = 0.3s (Δx = .0025). (a). Velocity (b). Velocity results by 2nd order Godunov [15] (c). Pressure (d). Density (e). Temperature (f). specific heat ratio

The initial discontinuity at X = 0.25 generates a rarefaction wave which moves towards left and a shock wave which moves towards the right and strikes the slab of the helium gas at X = 0.5. The shock wave interaction with the helium slab results in a partial reflection of the wave into the region of air and a partial refraction of the shock wave into the helium region. The multi-fluid model successfully incorporates all the wave interactions to generate the results. First order Godunov scheme is dissipative (Figure 21(a)) and it may not always be possible to simulate accurate results with the first order scheme. Second-order Godunov scheme (Figure 21(b)) can be used to improve the accuracy of the results by decreasing the dissipation. Figure 21(b) is the velocity profile obtained from the source reference paper by Wang et al. [15] and it has been compared with the velocity profile obtained with the 1st order Godunov scheme.

Case 3: This test case has been formulated to produce a weak post-shock contact discontinuity by hitting a material interface with a strong shock wave. The shock tube consists of a stationary interface at x = 0.5 m separating argon and nitrogen, and a right traveling shock wave (Mach number = 3.352) initially located at x = 0.25 m. The initial conditions and properties are defined as

$(\rho, u, p, \gamma, C_v = 5.10970, 738.6, 1398737, 1.67, 208.1)$ $\quad 0.00 < x < 0.25$

$(\rho, u, p, \gamma, C_v = 1.62286, 0.000, 0101325, 1.67, 208.1)$ $\quad 0.25 < x < 0.50$

$(\rho, u, p, \gamma, C_v = 1.13802, 0.000, 0101325, 1.40, 296.8)$ $\quad 0.50 < x < 1.00$

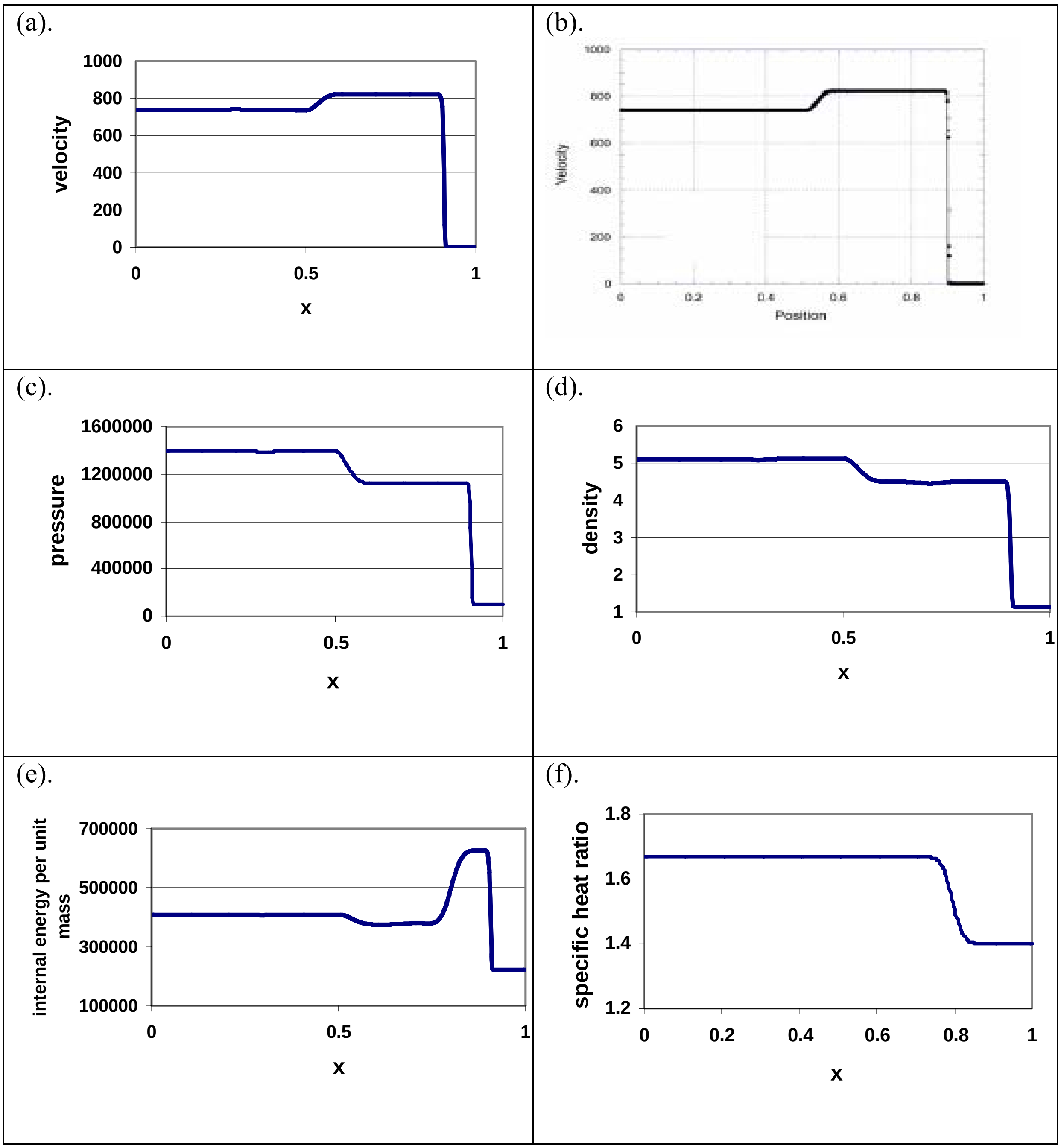

Fig 22: Results for Case 3 after time t = 600 μs (Δx=.0025). (a). Velocity (b). Velocity results by Wang et al.[15] (b). Pressure (c). Density (d). Temperature (e). specific heat ratio

The results for case 3 have been accurately simulated by the multi-fluid model and have been compared with the results by Wang et al. (Figure 22(b)) [15]. The shock wave (at X = 0.90), the contact discontinuity wave (at X = 0.80) and the rarefaction wave (*Head* at X = 0.56 and *Tail* at X = 0.50) can be seen in the results in the figure 21. Across the shock wave, velocity jumps from 800 m/s to 0 m/s (Figure 22(a)), pressure jumps from 1150000 N/m^2 to 101325 N/m^2 (Figure 22(c)), density jumps from 4.50 Kg/m^3 to 1.14 Kg/m^3 (Figure 22(d)) and the internal energy per unit mass jumps from 625000 J/Kg to 220000 J/ Kg (Figure 22(e)). Internal energy jumps from 380000 J/Kg to 625000 J/ Kg across the contact discontinuity wave (Figure 22(e)). This test also benchmarks the compressible multi-fluid model.

Case 4: This shock-contact surface interaction problem has been studied to verify the convergence of numerical solutions to the correct weak ones. A stationary interface (at x = 0.5) problem is considered here where the interface separates two different gases. The initial states are defined as

$(\rho_L, u_L, p_L, \gamma_L =$ 1.0, 0.00, 10.0, 1.6) $\quad x < 0.5$

$(\rho_R, u_R, p_R, \gamma_R =$ 2.0, -1.0, 0.10, 1.4) $\quad x > 0.5$

The results for the case 4 are shown in the figure 23. The shock wave (at X = 0.83) and the contact discontinuity wave (at X = 0.66) have been accurately simulated by the multi-fluid model. Across the shock wave, velocity jumps from 0.73 to -1.00 (Figure23(a)), pressure jumps from 7.40 to 0.10 (Figure 23(b)), density jumps from 11.30 to 2.00 (Figure 23(c)) and the internal energy per unit mass jumps from 1.64 to 0.13 (Figure 23(d)). Internal energy per unit mass jumps from 15 to 1.64 and density jumps from 0.90 to 10.30 across the contact discontinuity wave. This is another test to benchmark the compressible multi-fluid model.

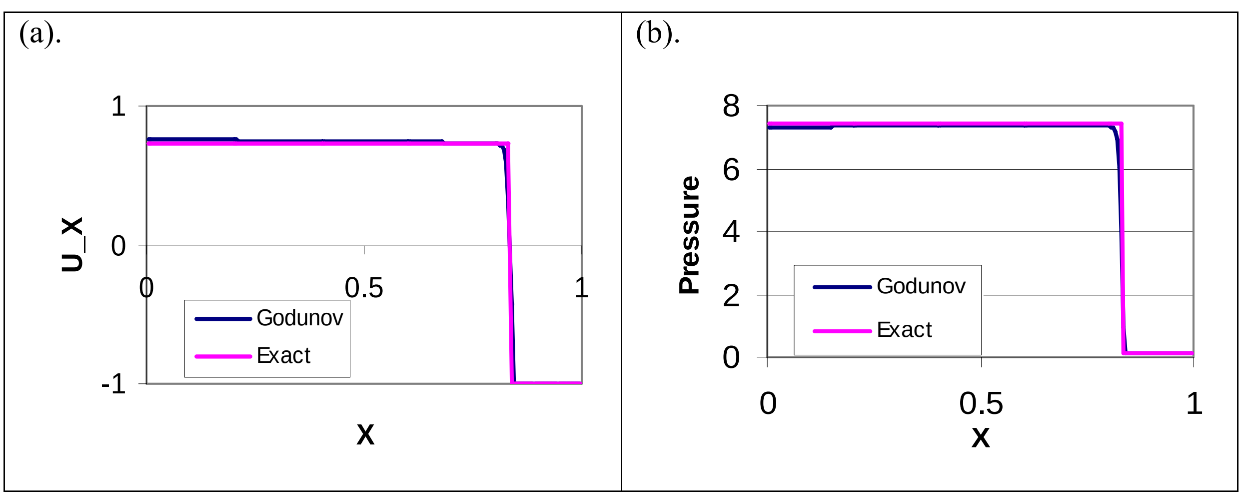

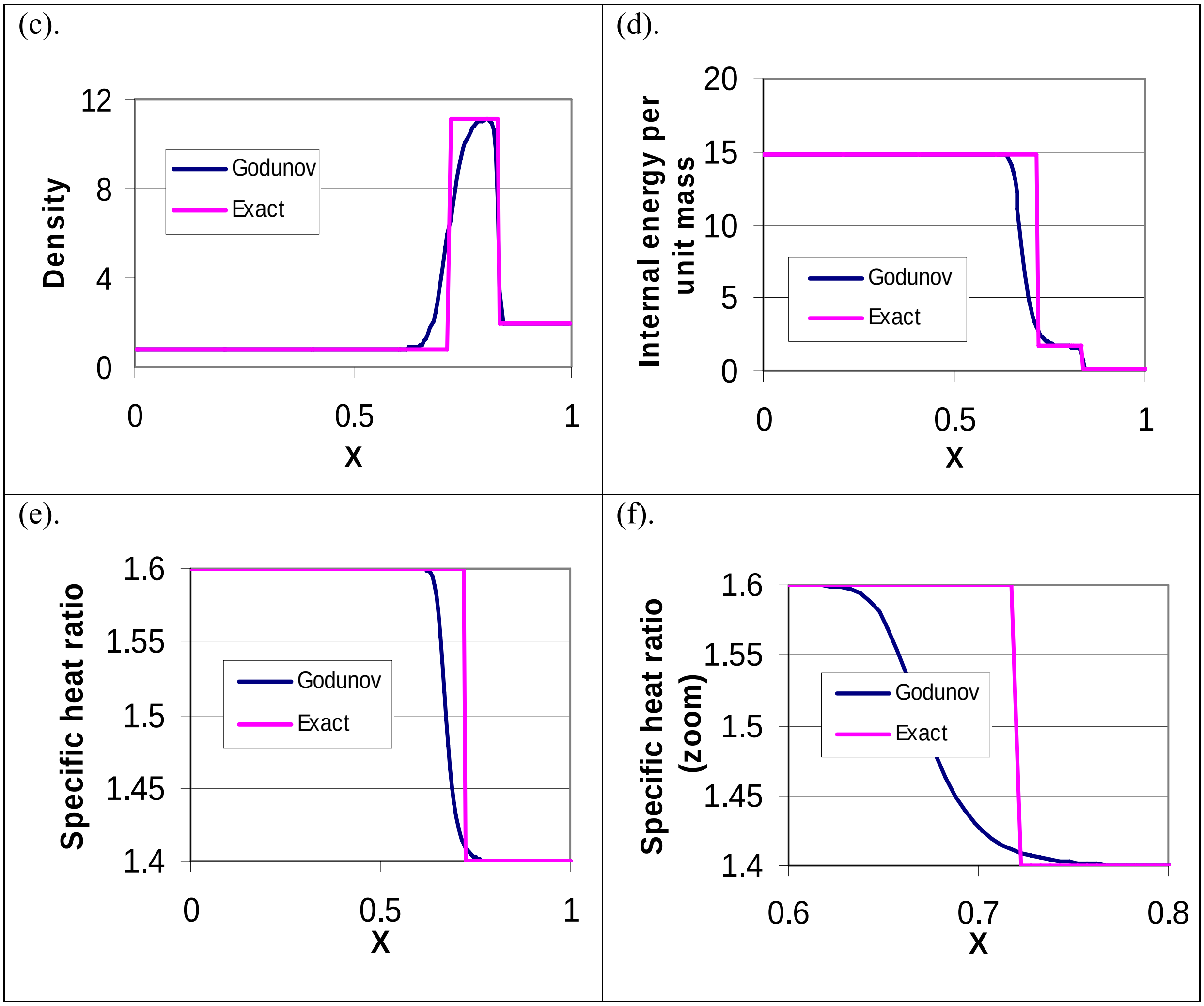

Fig 23: Results for Case 4 after time t = 0.3 (Δx = .005). (a). Velocity (b). Pressure (c). Density (d). Temperature (e). specific heat ratio (f). zoomed specific heat ratio

Case 5: The different gases in the two sections of the tube are separated by a diaphragm. The initial parameters on left and right side of the diaphragm are,

$(\rho_L, u_L, T_L, \gamma_R, R_L = 1, 0, 1, 1.40, 1.0)$ $\qquad x < 0$

$(\rho_R, u_R, T_R, \gamma_R, R_R = 5, 0, 1, 1.28, 0.8)$ $\qquad x > 0$

Comparison between the results obtained from the new hybrid FVM-LBM method, FVM along with the Godunov scheme and the exact solution has been shown in figure 24. The results show that the new method gives a more accurate shock profile than the profile obtained with the FVM for compressible multi-fluid flows. The new method also gives a significantly higher computational efficiency as the LBM, which is a non-iterative procedure, is used to compute the inter-cell parameters. The robust hybrid method incorporates the advantages of both FVM and LBM and this test case shows that the FVM–LBM method is effective for multi-fluid flows also.

(a).

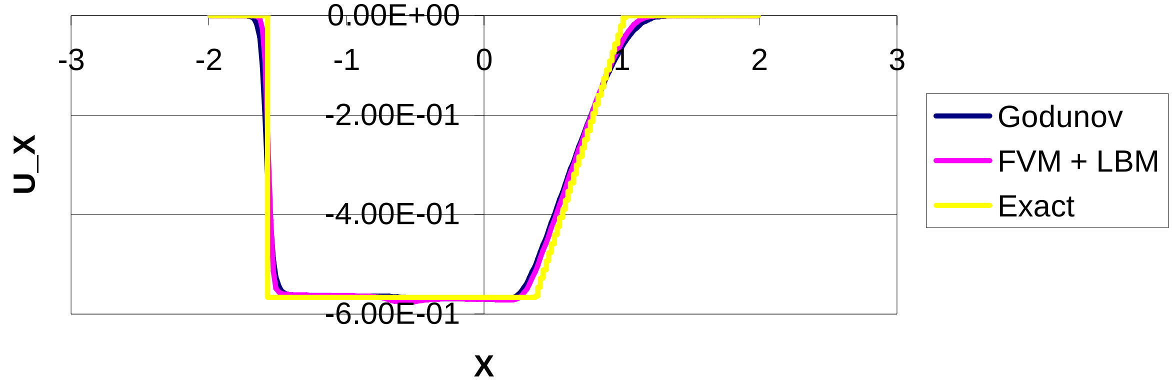

(b).

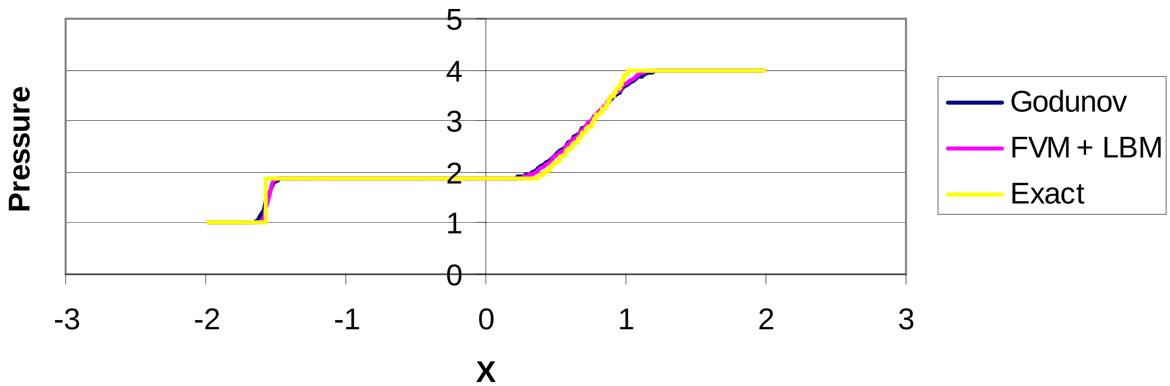

(c).

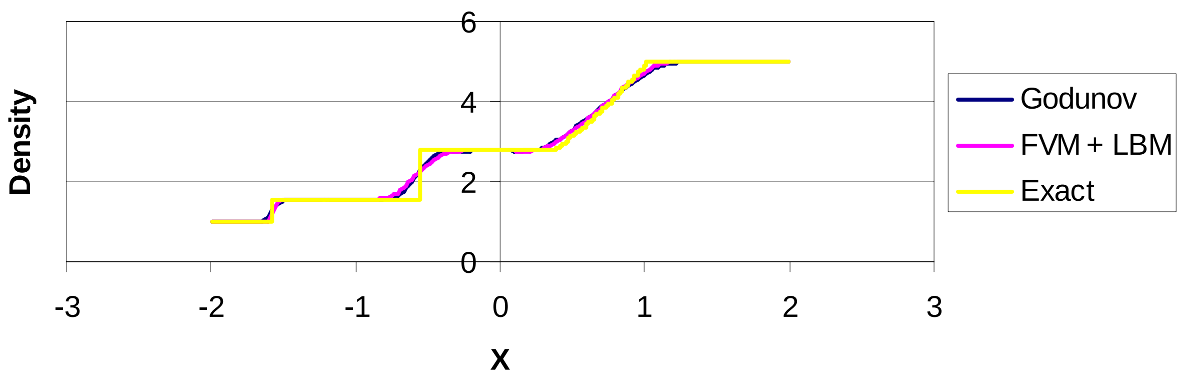

(d).

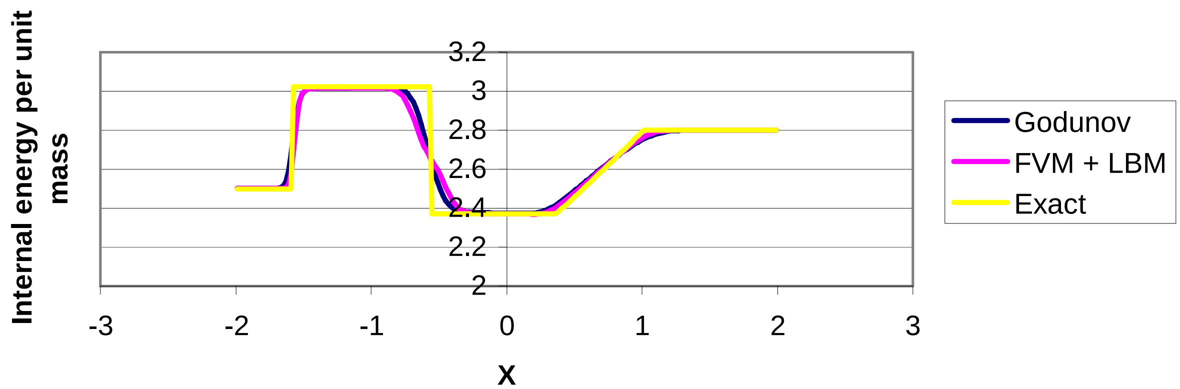

(e).

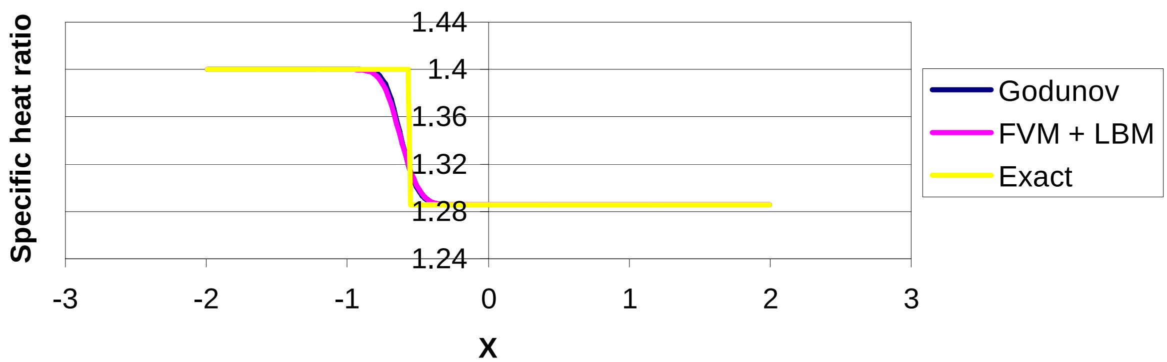

Fig 24: Results for Case 5 after time t = 1 (Δx = .02). (a). Velocity (b). Pressure (c). Density (d). Temperature (e). Specific heat ratio

All the three waves (shock wave, contact discontinuity wave and expansion fan wave) have been accurately simulated by the new method. The jumps across the shock wave in pressure, density and internal energy per unit mass are 1.90, 1.57 and 3.02 respectively (Figure 24(b), 24(c), 24(d)). The contact discontinuity wave moves at a speed of 0.57 towards the left of initial discontinuity (Figure 24(e)) which is equal to the velocity drop across the shock wave. The internal energy per unit mass drops from 3.02 to 2.37 and density increases from 1.57 to 2.79 across the contact discontinuity. The new method simulates more accurate shock wave (at X = -1.57), contact discontinuity wave (at X = -0.57) and expansion fan (*Head* at X = 1.03 and *Tail* at X = 0.37) as compared to the results obtained by FVM along with the Godunov scheme. The computation time required by the new hybrid method (35.22 s) is about 23% less than the time required by FVM along with Godunov scheme (43.35 s).

7.5 Results from the hybrid FVM-LBM method with non-uniform grid

One of the limitations of Lattice Boltzmann method is that it can only be used with uniform grids. Finite Volume Method on the other hand can be used with non-uniform grids also. The new hybrid FVM-LBM method which is a combination of FVM and LBM can be used with non-uniform grids. The results obtained for the shock tube problem with the hybrid method using a non-uniform grid are shown in the figure 25. The entire domain is divided into 250 node points. The grid spacing i.e. the spacing between two nodes is alternatively set as 0.01 and 0.03. A comparison between the results obtained with the hybrid FVM-LBM method, pure FVM along with the use of Godunov scheme and the exact solution shows that the hybrid method can be effective with non-uniform grids also.

(a).

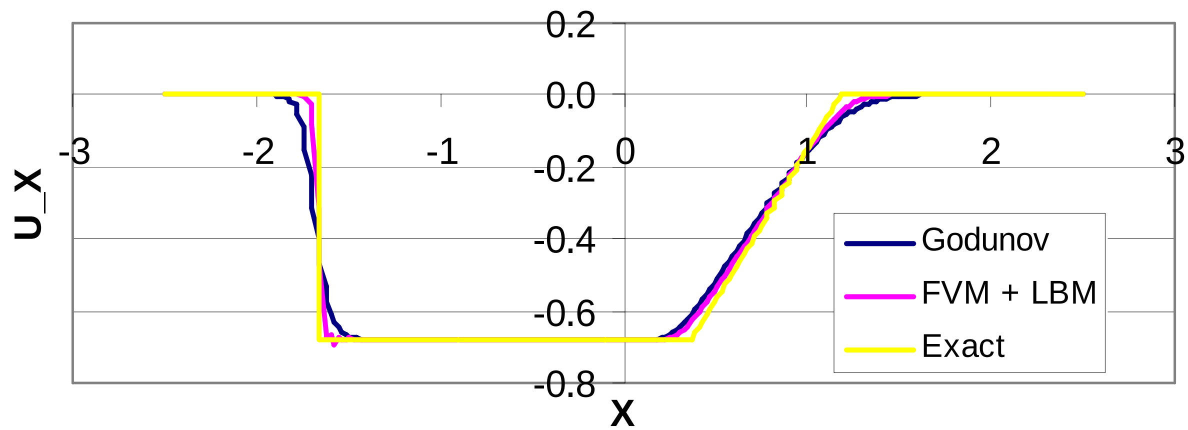

(b).

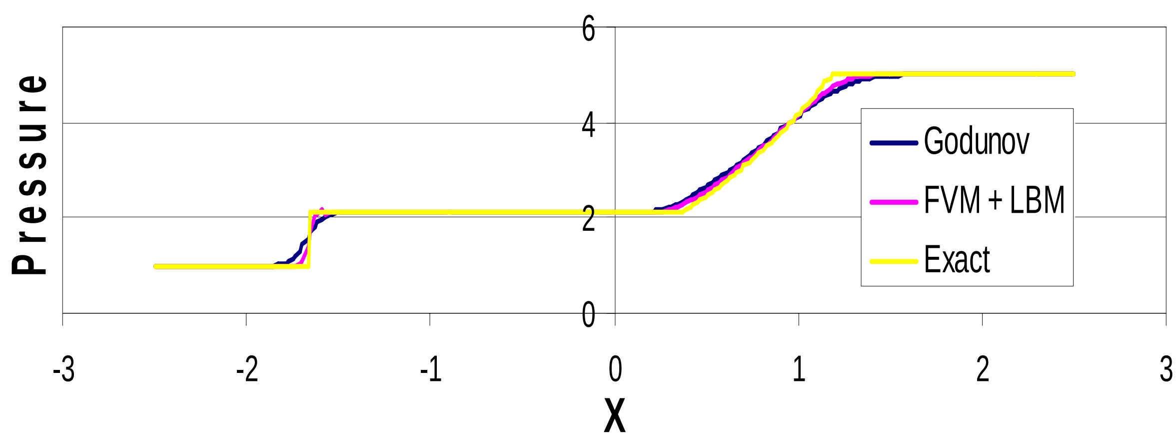

(c).

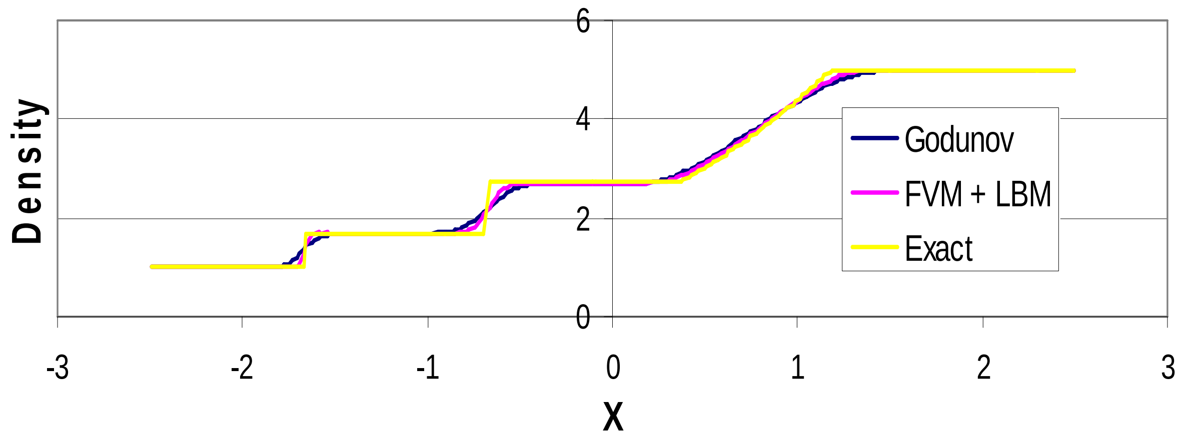

(d).

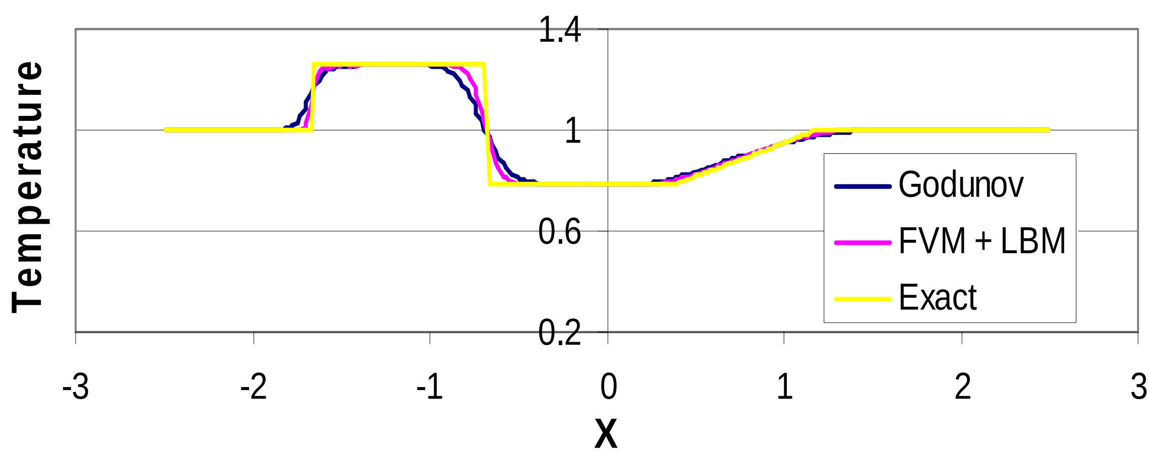

Fig 25: Results for Shock Tube problem with non-uniform grid after time t = 1 (ε = .001, γ = 1.4) (a). Velocity (b). Pressure (c). Density (d). Temperature

The new method is accurate and computationally more efficient with non-uniform grids also. The profiles for velocity (Figure 25(a)), pressure (Figure 25(b)), density (Figure 25(c)), and temperature (Figure 25(d)) show that the hybrid method generates more accurate shock and contact discontinuity profiles than the Godunov scheme with non-uniform grids. Computational time has also been significantly reduced by the hybrid method with the non-uniform grid. Thus, the hybrid method overcomes the limitation of LBM which can only be used with uniform grid.

Chapter 8

Conclusions

It has been established that the newly proposed hybrid FVM-LBM method is capable of simulating steep and accurate shock and contact discontinuity profiles in comparison with the conventional methods for solving Euler equations i.e. FVM along with Godunov scheme to simulate the inter-cell parameters from the node parameters. This scheme also overcomes one of the main drawbacks of LBM as it can also be used with non-uniform mesh. At the same time this scheme is computationally efficient and reduces processing time by around 22%. One of the limitations of LBM proposed by Kataoka and Tsutahara is that local Mach number has to be less than 1. Therefore, the new hybrid method will also be affected by this limitation and alternative LBM models can help to overcome this limitation.

A computational solver has also been developed for the multi-fluid model proposed by Wang et al.. This model has been benchmarked for a few standard test cases. The new hybrid method has been used to simulate the shock tube problem with different gases on the either side of initial discontinuity. The new hybrid method is again computationally more efficient and produces accurate shock profile when compared with the Godunov scheme. Thus, the new hybrid FVM–LBM method for compressible Euler equations appears to be a robust numerical method which incorporates the advantages of both Finite Volume method and Lattice Boltzmann method.

References

1. A. W. Date, "*Introduction to Computational Fluid Dynamics*", 1st Edition, Cambridge University Press, 2005

2. E.F. Toro, "*Riemann Solvers and Numerical Methods for Fluid Dynamics",* 2nd Edition, Springer Publication, 1999

3. S. Succi, "*The Lattice Boltzmann Equation for Fluid Dynamics and Beyond",* 1st Edition, Oxford Science Publication, 2001

4. T. Kataoka, M. Tsutahara, "*Lattice Boltzmann method for compressible Euler equations",* Physical Review E, Volume 69, 056702, 2004

5. P. D. Lax, B. Wendroff, "*System of conservation laws*", Commun. Pure Applied Mathematics, 13:217-237, 1960

6. S. Godunov, *"A finite difference method for the computation of discontinuous solutions of the equations of Fluid Dynamics*", Math. Sbornik, 47:357-393, 1959

7. P. Roe, "*Approximate Riemann solvers, parameter vectors, and difference schemes*", Journal of Computational Physics, 43:357-372, 1981

8. P. Roe and J. Pike, "*Efficient construction and utilization of approximate Riemann solutions*", In Computing Methods in Applied Science and Engineering, North-Holland, 1984

9. A. Harten, P. Lax, B. van Leer, "*On upstream differencing and Godunov-type schemes for hyperbolic conservation Laws*", Journal of Computational Physics, 50:235-269, 1983

10. E. F. Toro, M. Spruce, and W. Spears, "*Restoration of the contact surface in the HLL-Riemann solver*", Shock Waves, 4:25-34, 1994

11. F. Alexander, S. Chen, J. Sterling, "*Lattice Boltzmann Thermohydrodynamics*", Physical Review E, Volume 47, 2249, 1993

12. Alexander et al., "*Lattice Boltzmann method for compressible fluids*", The American Physical Society Vol. 46, pp 1967-1970, 1992

13. H. Yu, K. Zhao, "*Lattice Boltzmann method for compressible flows with high mach number*", The American Physical Society Vol. 61, pp 3867-3870, 2000

14. Y. Guangwu, C. Yaosong, H. Shouxin, *"Simple Lattice Boltzmann model for simulating flows with shock wave"*, Physical Review E, Volume 59, No. 1, 1999

15. Wang et al., "*A thermodynamically consistent and fully conservative treatment of contact discontinuities for compressible multi-component flows"*, Journal of Computational Physics 195, 528-559, 2004

16. J.D. Anderson, "*Modern Compressible Flow",* 3rd Edition, Mc. Graw Hill Publications, 2003

17. Y. H. Qian, "*Simulating thermodynamics with Lattice BGK* models", Journal of Scientific Computing, Volume 8, 231-242, 1993

18. P. Bhatnagar, E. Gross, M. Krook, "*A model for collision processes in gases. I. small amplitude processes in charged and neutral one-component systems*", Physical Review 94, 511-525. 1954

19. Website: http://amroc.sourceforge.net/

Novel LBM Scheme for Euler Equations

Arpit Agarwal[1], **Amit Agrawal**[1], **Bhalchandra Puranik**[1], **and Chang Shu**[2]

[1] *Department of Mechanical Engineering, Indian Institute of Technology-Bombay, India.*
[2] *Department of Mechanical Engineering, National University of Singapore, Singapore.*

Summary. Lattice Boltzmann Method (LBM) as a relatively new numerical method has recently achieved considerable success in simulating compressible fluid flows. A hybrid method, which is a combination of the usual Finite Volume Method (FVM) and the LBM, is proposed here to solve the Euler Equations. The inter-cell parameters are obtained by solving the local Riemann problem for each inter-cell using LBM. LBM is a non-iterative process and is thus numerically inexpensive as compared to the Godunov scheme. The proposed scheme is benchmarked for several 1-D problems such as the shock tube problem, the Roe test and the Riemann problem. The results obtained using this hybrid method are compared with those obtained using the Godunov scheme.

1 Introduction

Lattice Boltzmann Method (LBM) has developed as an alternative and promising numerical technique for simulating fluid flows, e.g., [1],[2],[3]. Boltzmann equation is solved to simulate the fluid flow using collision models such as the Bhatnagar-Gross-Krook (BGK) model [4]. The method is computationally less expensive and the boundary conditions can be easily implemented to get high accuracy [5]. It is very effective even with complex boundaries [6] and can also simulate steep shock and contact discontinuity profiles. One of the biggest disadvantages of LBM is that it cannot be used with a non-uniform mesh. FVM along with the use of the Godunov scheme to obtain the interface parameters has been widely used to simulate Euler equations [7]. The key ingredient of this scheme is the solution of a Riemann problem. There is no closed-form solution to the Riemann problem and iterative methods such as the Newton Raphson method are used to obtain the solution. FVM can be used with non-uniform mesh but the use of iterative schemes to obtain the solution of Riemann problem makes the method computationally expensive.

The proposed hybrid method in the present work solves the Euler equations using FVM with the solution to the Riemann problem being obtained by LBM. We employ the compressible perfect gas LB model proposed by Kataoka and Tsutahara [8]. This model allows for the free choice of specific heat ratio. LBM is a non-iterative solver for the Riemann problem and is therefore expected to be more efficient than Godunov scheme. Thus the hybrid method is expectecd to incorporate the advantages of both FVM and LBM.

2 Non-dimensional form of the Euler equations

All variables and equations are expressed in their non-dimensional form for the convenience of numerical calculations and analysis. Let L, ρ_{R0}, and T_{R0} respectively be the reference length, density and temperature. Then the other non-dimensional variables are defined as

$$t = \frac{\hat{t}}{L/\sqrt{RT_{R0}}},\ x = \frac{\hat{x}}{L},\ y = \frac{\hat{y}}{L} \tag{1}$$

$$\rho = \frac{\hat{\rho}}{\rho_{R0}},\ u_x = \frac{\hat{u_x}}{\sqrt{RT_{R0}}},\ u_y = \frac{\hat{u_y}}{\sqrt{RT_{R0}}},\ T = \frac{\hat{T}}{T_{R0}},\ p = \frac{\hat{p}}{\rho_{R0} RT_{R0}}. \tag{2}$$

The symbol ($\hat{}$) indicates a parameter in its dimensional form.

The two-dimensional time-dependent Euler equations in differential form are

$$U_t + F(U)_x + G(U)_y = 0, \tag{3}$$

where U, F(U) and G(U) are the vectors of conserved variables and fluxes given by

$$U = \begin{bmatrix} \rho \\ \rho u_x \\ \rho u_y \\ E \end{bmatrix},\ F(U) = \begin{bmatrix} \rho u_x \\ \rho u_x^2 + p \\ \rho u_x u_y \\ u_x(E+p) \end{bmatrix},\ G(U) = \begin{bmatrix} \rho u_y \\ \rho u_x u_y \\ \rho u_y^2 + p \\ u_y(E+p) \end{bmatrix}. \tag{4}$$

E (total internal energy per unit volume) is given by

$$E = \rho[0.5(u_x^2 + u_y^2) + e]. \tag{5}$$

Equation of state is given by

$$p = \rho T. \tag{6}$$

A conservative scheme for Eq. 3 is of the form

$$U_{(i,j)}^{n+1} = U_{(i,j)}^{n} + \frac{\Delta t}{\Delta x}[F_{i-1/2} - F_{i+1/2}] + \frac{\Delta t}{\Delta y}[G_{i-1/2} - G_{i+1/2}], \tag{7}$$

where $U_{(i,j)}^n$ denotes the parameters at the node (i,j) and at time interval n. The inter-cell numerical fluxes F and G are computed using the solution of local Riemann problem. Instead of solving the local Riemann problem in an iterative manner, the LBM scheme is used to calculate inter-cell parameters.

3 LBM scheme for compressible Euler equations

LBM proposed by Kataoka and Tsutahara is used to simulate the inter-cell parameters at the new time step from the known cell and inter-cell parameters at the earlier time step. The solution procedure is non-iterative and is expected to be more efficient than the Godunov scheme where the analytical solution of the local Riemann problem is obtained by iterative procedure.

We now present a synopsis of the LB model developed by Kataoka and Tsutahara. In the Lattice Boltzmann model, the macroscopic variables density, velocity and temperature are defined in terms of a particle velocity distribution function (f_i) as:

$$\begin{cases} \rho = \sum_{1\le i\le I} f_i, \\ \rho u_x = \sum_{1\le i\le I} f_i c_{xi}, \\ \rho u_y = \sum_{1\le i\le I} f_i c_{yi}, \\ \rho[bT + u_x^2 + u_y^2] = \sum_{1\le i\le I} f_i[c_{xi}^2 + c_{yi}^2 + \eta_i^2]. \end{cases} \tag{8}$$

Here, c_{xi} and c_{yi} are the molecular velocities of the particle moving in i^{th} direction (i = 1,2, ..., $I = 9$) and η_i is another variable which has been introduced to control the specific heat ratio. b is a constant which is expressed in terms of specific heat ratio (γ) as

$$b = \frac{2}{\gamma - 1}. \tag{9}$$

The kinetic equation of the non-dimensional form is

$$\frac{\partial f_i}{\partial t} + c_{xi}\frac{\partial f_i}{\partial x} + c_{yi}\frac{\partial f_i}{\partial y} = \frac{f_i^{eq}(\rho, u_x, u_y, T) - f_i}{\epsilon}, \tag{10}$$

where ϵ is the Knudsen number and the distribution function at the old time step is obtained from the equilibrium distribution function, i.e.,

$$f_i^0 = f_i^{eq}(\rho^0, u_x^0, u_y^0, T^0). \tag{11}$$

The two-dimensional Lattice Boltzmann Model is now presented:

$$(c_{xi}, c_{yi}) = \begin{cases} (0,0) & (i = 1) \\ v_1(\cos\frac{\pi i}{2}, \sin\frac{\pi i}{2}) & (i = 2,3,4,5) \\ v_2(\cos\frac{\pi(i+.5)}{2}, \sin\frac{\pi(i+.5)}{2}) & (i = 6,7,8,9) \end{cases} \tag{12}$$

and

$$\eta_i = \begin{cases} \eta_0 & (i = 1) \\ 0 & (i = 2,3,...9) \end{cases} \tag{13}$$

where v_1, v_2 ($v_1 \neq v_2$) and η_0 are non-zero constants.

The local equilibrium velocity distribution function is defined as

$$f_i^{eq} = \rho(A_i + B_i(u_x c_{xi} + u_y c_{yi}) + D_i(u_x c_{xi} + u_y c_{yi})^2) \quad (i = 1,2,3,...9) \tag{14}$$

where

$$A_i = \begin{cases} \frac{b-2}{\eta_0^2}T & (i = 1) \\ \frac{1}{4(v_1^2 - v_2^2)}[-v_2^2 + ((b-2)\frac{v_2^2}{\eta_0^2} + 2)T + \frac{v_2^2}{v_1^2}(u_x^2 + u_y^2)] & (i = 2,3,4,5) \\ \frac{1}{4(v_2^2 - v_1^2)}[-v_1^2 + ((b-2)\frac{v_1^2}{\eta_0^2} + 2)T + \frac{v_1^2}{v_2^2}(u_x^2 + u_y^2)] & (i = 6,7,8,9) \end{cases} \tag{15}$$

$$B_i = \begin{cases} \frac{-v_2^2+(b+2)T+u_x^2+u_y^2}{2v_1^2(v_1^2-v_2^2)} \ (i = 2,3,4,5) \\ \\ \frac{-v_1^2+(b+2)T+u_x^2+u_y^2}{2v_2^2(v_2^2-v_1^2)} \ (i = 6,7,8,9) \end{cases} \tag{16}$$

$$D_i = \begin{cases} \frac{1}{2v_1^4} \ (i = 2,3,4,5) \\ \\ \frac{1}{2v_2^4} \ (i = 6,7,8,9) \end{cases} \tag{17}$$

The parameters in Eq. 12 and Eq. 13 are chosen to be $v_1 = 1$, $v_2 = 3$, $\eta_0 = 2$. Discretized form of Eq. 10 is used to determine the new inter-cell parameters from the old node and inter-cell parameters in a single time step. In the present work the discretization employed is first order forward in time and first order upwind in space.

4 Results

The hybrid method has been numerically benchmarked against several test cases. These include several one-dimensional initial value problems (IVP) in gas dynamics, demonstrating the generation and propagation of shock waves, rarefaction waves and contact discontinuity waves. Specific heat ratio of the gas in all cases is 1.4 (or $b = 5$) and the time step is set at $\Delta t = \epsilon/4$. All results from this hybrid scheme have been compared with the exact solutions and the results obtained from Godunov scheme.

4.1 The shock tube problem

The rupture of a diaphragm which separates two stationary gases generates a wave system that typically consists of a rarefaction wave, a contact discontinuity and a shock wave. The initial variables of shock tube problem are given by

$$(\rho_L, u_L, T_L) = (1, 0, 1) \quad (x < 0),$$
$$(\rho_R, u_R, T_R) = (5, 0, 1) \quad (x > 0).$$

The pressure and the density profiles within the shock tube at a non-dimensionalized time, $t = 1$, are shown in Fig. 1. It can be noted that the hybrid scheme is able to capture the wave structure more accurately as compared with the FVM with Godunov scheme.

4.2 The Riemann problem

The Riemann problem is a slight generalization of the shock tube problem in the sense that the two gases on either side of the diaphragm may not be stationary. The given initial conditions generates a centered wave function which consists of two shock waves. The initial variables of Riemann problem are given by

$$(\rho_L, u_L, T_L) = (1, 1, 1) \quad (x < 0),$$
$$(\rho_R, u_R, T_R) = (1, -1, 1) \quad (x > 0).$$

The pressure and the density profiles within the one-dimensional domain at a non-dimensionalized time, $t = 1$, are shown in Fig. 2. It can again be noted that the hybrid scheme is able to capture the wave structure more accurately as compared with the FVM with Godunov scheme.

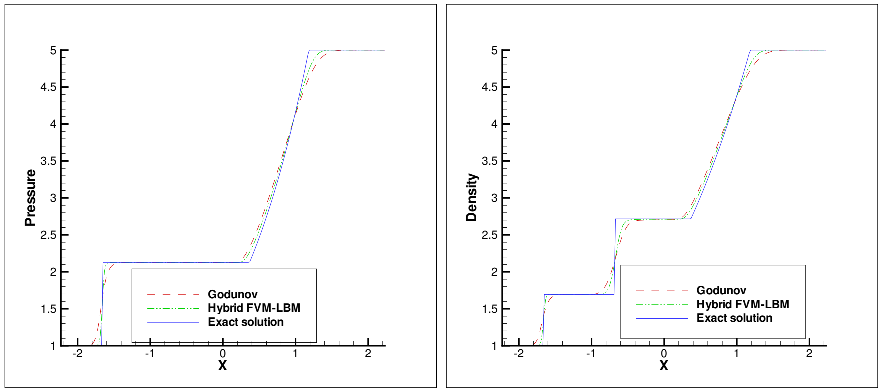

Fig. 1. Shock tube problem: pressure and density profile at $t = 1$ ($\Delta x = 0.02$; $\epsilon = 0.001$)

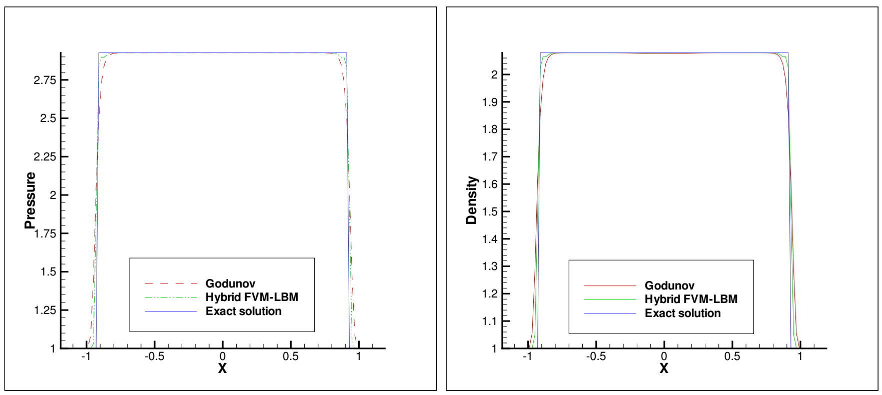

Fig. 2. Riemann problem: pressure and density profile at $t = 1$ ($\Delta x = 0.02$; $\epsilon = 0.001$)

4.3 The Roe test

The given initial condition generates a centered wave function which consists of rarefaction waves. The initial variables of Roe test are given by

$$(\rho_L, u_L, T_L) = (1, -1, 1.8) \qquad (x < 0),$$

$$(\rho_R, u_R, T_R) = (1, 1, 1.8) \qquad (x > 0).$$

The pressure and density profiles within the one-dimensional domain at a non-dimensionalized time, $t = 0.2$, are shown in Fig. 3. Once again it is seen that the hybrid scheme is able to capture the wave structure more accurately as compared with the FVM with Godunov scheme.

5 Conclusion

A hybrid method which is a combination of FVM and LBM is presented. The benchmarking tests show that the hybrid FVM-LBM scheme simulates the shock and contact discontinuity profile more accurately as compared to the profiles simulated by the

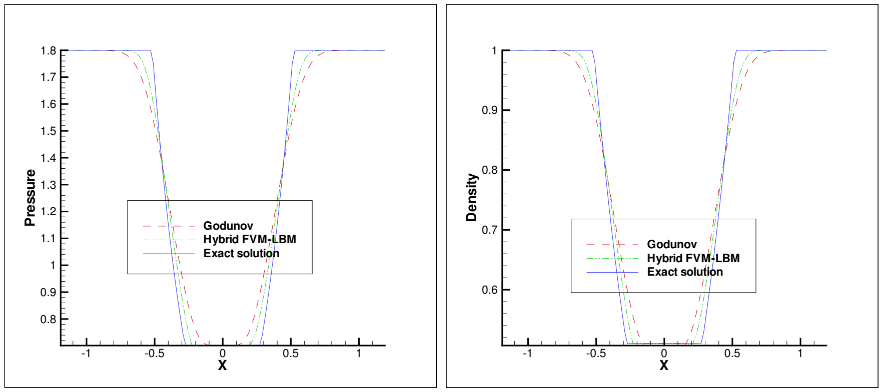

Fig. 3. Roe test: pressure and density profile at $t = 0.2$ ($\Delta x = 0.02$; $\epsilon = 0.001$)

Godunov scheme. The new scheme is computationally very efficient and this is clearly indicated by the reduced processing times as shown in the Table 1. In order to clearly determine the computational efficiency and accuracy, the hybrid scheme is required to be employed to simulate multidimensional problems; such efforts are underway.

Table 1. Comparison of processing times for the FVM-LBM scheme and the Godunov scheme

Benchmarking tests	FVM-LBM hybrid scheme	Godunov scheme
Shock tube problem	33.63 seconds	45.71 seconds
Riemann problem	34.78 seconds	46.44 seconds
Roe test (time = 0.2)	7.19 seconds	8.50 seconds

References

1. Succi S.: *The Lattice Boltzmann Equation for Fluid Dynamics and Beyond*, Numerical Mathematics and Scientific Computation, Oxford University Press, 2001.
2. Hudong Chen, Shiyi Chen, Matthaeus, W.H., Recovery of Navier-Stokes equations using a lattice-gas Boltzmann method, Physical Review A, **45**, 8, 5339-5342, 1992.
3. McNamara G. R., Zanetti G., Use of the Boltzmann equation to simulate lattice-gas automata, Physical Review Letters, **61**, 20, 2332-2335, 1988.
4. Bhatnagar P. L., Gross E. P., Krook M., A model for collision processes in gases. I. small amplitude processes in charged and neutral one-component systems, Physical Review, **94**, 3, 511-525, 1954.
5. Maier R. S., Bernard R. S., Grunau D. W., Boundary conditions for the Lattice Boltzmann method, Physics of Fluids, **8**, 7, 1788-1801, 1996.
6. Guo Z., Zheng C., Shi B., An extrapolation method for boundary conditions in Lattice Boltzmann method, Physics of Fluids, **14**, 6, 2007-2010, 2002.
7. Toro E. F.: *Riemann Solvers and Numerical Methods for Fluid Dynamics*, 2^{nd} Edition, Springer Publication, 1999.
8. Kataoka T., Tsutahara M., Lattice Boltzmann method for the compressible Euler equations, Physical Review E, **69**, 056702, 2004.